Antagonists of the Calcium Receptor I. Amino Alcohol-Based Parathyroid Hormone Secretagogues

Robert W. Marquis,*[,†] Amparo M. Lago,[†] James F. Callahan,[†] Robert E. Lee Trout,[†] Maxine Gowen,[‡] Eric G. DelMar,[#] Bradford C. Van Wagenen,[#] Sarah Logan,[#] Scott Shimizu,[#] John Fox,[#] Edward F. Nemeth,[#] Zheng Yang,[||] Theresa Roethke,[§] Brian R. Smith,[§] Keith W. Ward,[§] John Lee,[⊥] Richard M. Keenan,[†] and Pradip Bhatnagar[†]

Departments of Medicinal Chemistry, Bone and Cartilage Biology, Drug Metabolism and Pharmacokinetics, Computational and Structural Chemistry, and Cellular Biochemistry, GlaxoSmithKline, 1250 South Collegeville Road, Collegeville, Pennsylvania 19426, NPS Pharmaceuticals, 550 Hills Drive, Bedminster, New Jersey 07921

Received March 23, 2009

Functional screening of the former SmithKline Beecham compound collection against the human calcium receptor (CaR) resulted in the identification of the amino alcohol-based hit **2** (IC_{50} = 11 μM). Structure−activity studies of **2** focused on the optimization of the right- and left-hand side aromatic moieties as well as the amino alcohol linker region. Critical to the optimization of this antagonist template was the discovery that the chirality of the C-2 secondary alcohol played a key role in enhancing both CaR potency as well as selectivity over the β-adrenergic receptor subtypes. These SAR studies ultimately led to the identification of **38** (NPS 2143; SB-262470A), a potent and orally active CaR antagonist. Pharmacokinetic characterization of **38** in the rat revealed that this molecule had a large volume of distribution (11 L/kg), which resulted in a prolonged systemic exposure, protracted increases in the plasma levels of PTH, and an overall lack of net bone formation effect in a rodent model of osteoporosis.

Downloaded by UNIV OF NEWCASTLE on October 11, 2009 | http://pubs.acs.org
Publication Date (Web): June 3, 2009 | doi: 10.1021/jm900364m

Introduction

Bone is a dynamically remodeling tissue balanced by the interplay of osteoclasts that degrade bone and osteoblasts that produce new bone. When the resorption phase of remodeling outpaces new bone formation, the overall architecture of bone is weakened, leading ultimately to osteoporosis.[1] There are currently several marketed drugs for the prevention and treatment of osteoporosis.[2] The vast majority of these therapeutics are antiresorptive agents and act to slow bone loss by inhibiting osteoclast activity. The bisphosphonates, estrogens, selective estrogen receptor modulators, salmon calcitonin, the receptor activator of NK-κB ligand (RANK-L[a]) monoclonal antibody denosumab, and the cathepsin K inhibitor odanacatib have all demonstrated antiresorptive activity in human clinical trials but offer little or no new bone building effect. Recently, a new pharmacological approach for the treatment of osteoporosis has been introduced to the marketplace. Daily subcutaneous injections of recombinant full-length human parathyroid hormone (PTH) 1-84 (Nycomed) or teriparatide, the recombinant N-terminal PTH 1-34 amino acid fragment (Lilly), stimulate new bone formation leading to a reversal of osteoporotic bone loss in postmenopausal women.[3] Both PTH and teriparatide exert their bone forming effects by activating PTH/PTHrP receptors on osteoblasts and osteoblast precursor cells.[4]

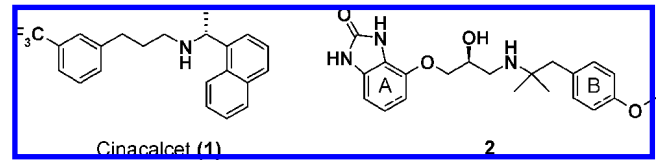

Figure 1. Calcimimetic cinacalcet (**1**) and antagonist screening hit **2**.

Another approach to the identification of a new bone forming therapeutic based upon the clinically validated mechanism of action of PTH and teriparatide, would be the development of an agent that would elicit the secretion of PTH from the parathyroid gland. PTH secretion is under the strict control of the calcium receptor (CaR), a family-C, cell surface G-protein coupled receptor that is capable of detecting minute variations in extracellular calcium ion concentrations (Ca^{2+}).[5] Elevation of extracellular Ca^{2+} concentrations activates the CaR and leads to a suppression of PTH secretion. Small molecule CaR agonists or allosteric activators, collectively known as calcimimetics, mimic elevated Ca^{2+} concentrations and inhibit PTH secretion.[6] Cinacalcet, *N*-[(1*R*)-1-(1-naphthalenyl)ethyl]-3-[3-(trifluoromethyl)phenyl]-1-propanamine, (**1**, Amgen/NPS, Figure 1) has therapeutic utility in controlling elevated PTH levels in patients with hyperparathyroidism, demonstrating that pharmacological manipulation of the CaR by a small molecule may be used in controlling PTH secretion.[7] In contrast to the inhibitory effects of high Ca^{2+} levels or calcimimetics on PTH secretion, low circulating Ca^{2+} levels stimulate PTH secretion. Small molecule antagonists of the CaR, known as calcilytics or negative allosteric modulators, mimic low extracellular Ca^{2+} and stimulate PTH secretion.[8−18]

An important aspect of the pharmacology of PTH and its agonist fragments is the temporal nature of the exposure to these

* To whom correspondence should be addressed. Phone: 1-610-917-7368. Fax: E-mail: Robert.W.Marquis@gsk.com. Address: Department of Medicinal Chemistry, ImmunoInflammation Center of Excellence in Drug Discovery, GlaxoSmithKline, 1250 South Collegeville Road, UP1110, Collegeville, PA 19426.

† Department of Medicinal Chemistry, GlaxoSmithKline.

‡ Department of Bone and Cartilage Biology, GlaxoSmithKline.

§ Department of Drug Metabolism and Pharmacokinetics, GlaxoSmithKline.

|| Department of Computational and Structural Chemistry, GlaxoSmithKline.

⊥ Department of Cellular Biochemistry, GlaxoSmithKline.

NPS Pharmaceuticals.

[a] Abbreviations: CaR, calcium receptor; PTH, parathyroid hormone; RANK, receptor activator of NK-κB; PTHrP, parathyroid hormone-related protein; HEK, human embryonic kidney; OVX, ovariectomized; SAR, structure−activity relationship; LDA, lithium diisopropylamide; DAT, dopamine transporter; SERT, serotonin transporter; NET, norepinephrine transporter; CYP2D6, cytochrome P450 2D6; hERG, human ether-a-go-go related gene; FLIPR, fluorimetric imaging plate reader.

10.1021/jm900364m CCC: $40.75 © 2009 American Chemical Society
Published on Web 06/03/2009

Downloaded by UNIV OF NEWCASTLE on October 11, 2009 | http://pubs.acs.org
Publication Date (Web): June 3, 2009 | doi: 10.1021/jm900364m

agents. Depending on the pattern of exposure PTH may act either as an anabolic agent, thereby building new bone, or as a catabolic agent, resulting in the loss of bone.[19] Prolonged exposure to PTH results in overall loss of bone as manifested in conditions such as hyperparathyroidism where PTH levels are elevated continuously. Alternatively, short intermittent exposure to elevated PTH or its fragments has an overall bone forming effect. This has been demonstrated with the daily subcutaneous administration of teriparatide which reaches T_{max} within 30 min, is rapidly cleared (62 L/h in women and 94 L/h in men) with a low volume of distribution (0.12 L/kg).[20] These results suggest that an orally active CaR antagonist would also have to have a pharmacokinetic/pharmacodynamic profile that is transient in nature in order to have a beneficial bone forming effect.

We have reported on the in vitro and in vivo pharmacodynamic effects of the amino alcohol-based CaR antagonist **38** (NPS 2143, SB-262470-A, Table 1).[8,9] When tested in human embryonic kidney 293 (HEK293) cells stably expressing the human CaR, analog **38** was potent (IC_{50} = 43 nM), it elicited PTH release from bovine parathyroid cells (EC_{50} = 41 nM), and it increased plasma PTH levels when infused iv in rats. In the osteopenic ovariectomized (OVX) rat **38** produced sustained elevations of plasma PTH following oral administration. The prolonged elevation in PTH levels led to increased bone turnover with no changes in bone mineral density following five weeks of treatment. When coadministered with 17β-estradiol, a known antiresorptive agent, an increase in bone mass was observed. In total, these data suggested that a short-acting, orally active PTH secretagogue may have a net bone forming effect and would represent a potential new treatment for postmenopausal osteoporosis.

This manuscript details the characterization of the first generation amino alcohol-based CaR antagonist hit **2** and some of the salient structure−activity relationship studies critical to the optimization of **2** that led to the identification of analog **38**.

Synthesis Chemistry. A functional assay was developed in HEK293 cells stably transfected with the human CaR to assess the ability of test compounds to block extracellular Ca^{2+}-induced increases in intracellular Ca^{2+}.[21] A high-throughput screen of the former SmithKline Beecham compound collection in this assay format led to the identification of the amino alcohol hit **2** (Figure 1, Table 1). In an effort to optimize the potency and selectivity of **2**, this molecule was divided into three separate regions to facilitate the systematic study of each of these areas structure−activity relationships (SAR) (Figure 1). These regions were the left-hand side benzimidazol-2-one group (designated A), the amino alcohol linking region and the right-hand-side aromatic group (designated B). The syntheses utilized to explore the SAR of each of these individual regions of **2** are detailed in Schemes 1−6.

The synthesis of the analogs designed to examine the SAR of the left-hand side aromatic moiety is detailed in Scheme 1. To facilitate analog synthesis the C2 racemic alcohols were utilized at this stage as the exact chirality of the C2 asymmetric center which was required for potent antagonism of the CaR had not yet been determined. Treatment of *iso*-butyric acid (**3**) with lithium diisopropylamide (LDA), followed by alkylation with *p*-methoxybenzyl chloride provided 2,2-dimethyl-3-[4-(methyloxy)phenyl]propanoic acid (not shown). This acid was then reacted with ethyl chloroformate, followed by sodium azide. The intermediate acyl azide was heated (100 °C) to effect Curtius rearrangement, and the isocyanate was captured with benzyl alcohol to yield the benzyl carbamate (not shown).

Scheme 1. Synthesis of Amino Alcohols by Varying the Left-Hand Side Moiety[a]

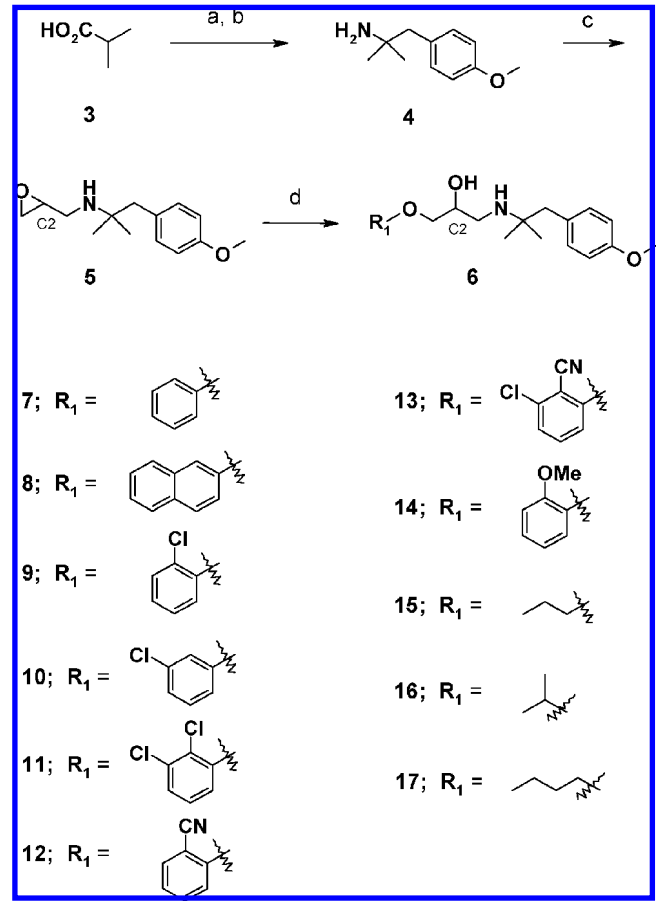

[a] Reagents and conditions: (a) LDA, HMPA, *i*-butyric acid, 4-methoxy benzylchloride, −78 °C to rt; (b) **3**, TEA, acetone, H_2O, ethyl chloroformate, NaN_3, 0 °C to rt then toluene 100 °C benzyl alcohol, EtOH, H_2, $Pd(OH)_2$; (c) *i*-PrOH, 0 °C, epichlorohydrin; (d) NaH, DMF, ROH, **5**, 100 °C.

Hydrogenolysis of the benzyl carbamate with hydrogen/palladium hydroxide gave (1,1-dimethyl-2-[4-(methyloxy)phenyl]-ethyl)amine (**4**). Treatment of amine **4** with epichlorohydrin provided the intermediate epoxide **5**, which was reacted with a variety of alkoxides to provide a range of left-hand side substituted analogs (**7**−**17**) for profiling against the CaR.

As outlined in Scheme 2, the synthesis of analogs designed to explore the SAR of the right-hand side aromatic moiety of **2** began with opening of 2-[(phenyloxy)methyl]oxirane (**18**) with a variety of different amines. The right-hand side amines contained within analogs **7**, **20**, **21**, and **22** were designed to explore the role of the *gem*-dimethyl group contained within **2**. Alternatively, analogs **23** and **24** were utilized to probe the optimal distance for the right-hand side aromatic group from the geminal-dimethyl moiety. Analogs **25** and **26** were incorporated in order to understand the potential role of the *p*-methoxy moiety and the extension of the π-aromatic system, respectively.

As outlined in Schemes 3 and 4, analogs **27** and **28** explored the role of the amino alcohol linker via either oxygen or nitrogen methylation. Treatment of **11** under standard Borsch reductive amination conditions (H_2CO, $NaCNBH_3$) provided the *N*-methylated analog **27** in 91% yield. Methylation of the hydroxyl moiety of **11** was accomplished by treatment of **11** with sodium hydride and methyl iodide to provide **28** in 49% yield. Alternatively, the role of the hydroxyl moiety was explored by simply removing this group from the amino alcohol antagonist

Scheme 2. Synthesis of Amino Alcohols by Varying the Right-Hand Side Moieties[a]

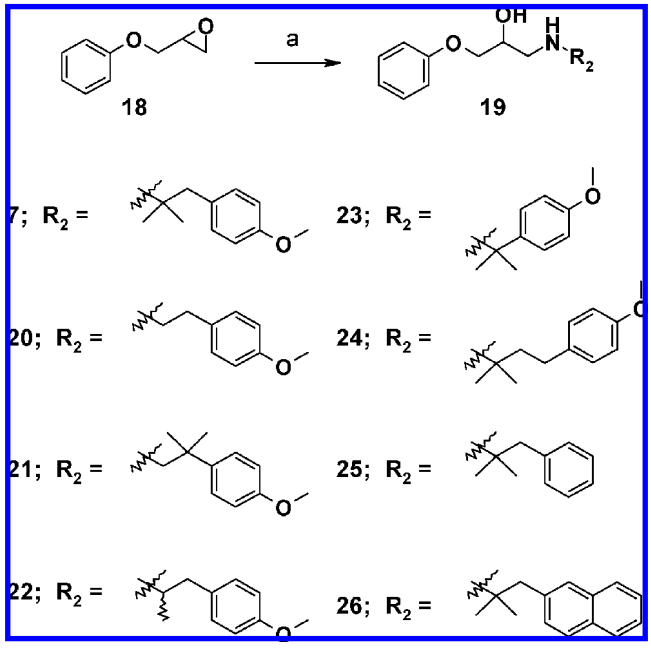

[a] Reagents and conditions: (a) RNH_2, EtOH, 80 °C.

template (Scheme 4). Alkylation of 2,3-dichlorophenol (**29**) with 1,2-dibromoethane provided the bromide **30** in 13% isolated yield. Displacement of the bromine with (1,1-dimethyl-2-[4-(methyloxy)phenyl]ethyl)amine (**4**) provided analog **31** in 28% yield.

In an effort to understand the role of the chirality of the C2 hydroxyl moiety as a function of antagonist potency and selectivty, the racemic alcohol **11** was separated via chiral HPLC to provide the enantiomerically pure *R* (faster eluting) and *S* (slower eluting) isomers **32** and **33**, respectively (Scheme 5). Assignment of the chirality of each of **32** and **33** was made possible through the chiral syntheses of each of these enantiomers beginning with the alkylation of 2,3-dichlorophenol (**29**) with the *R*- or *S*-nosyl epoxides to provide intermediates **34** and **35**, respectively. Treatment of the epoxides **34** and **35** with (1,1-dimethyl-2-[4-(methyloxy)phenyl]ethyl)amine (**4**) effected regiospecific ring-opening to provide the chiral amino alcohol antagonists **32** and **33**, respectively. Analogs **32** derived from the *R*-nosyl epoxide was shown to co-elute with the faster eluting of the two separated enantiomers, while analog **33** derived from the *S*-nosyl epoxide was shown to co-elute with the slower of the two enantiomers.

The syntheses of antagonists utilized to study the preliminary SAR studies described above have established some of the better left- and right-hand side aromatic moieties as well as the requisite *R* chirality of the secondary C2-hydroxyl group for antagonist activity as well as selectivity. In an effort to optimize antagonist potency each of these groups was incorporated in the amino alcohol template of the original hit **2**. As shown in Scheme 6, the syntheses of this optimized antagonist began with alkylation of 2-chloro-6-hydroxybenzonitrile (**36**) with *R*-nosyl epoxide to provide the chiral epoxide **37** with the C2-*R* stereochemistry. Regiospecific opening of this chiral epoxide with (1,1-dimethyl-2-(2-naphthalenyl)ethyl)amine provided antagonist **38**.

Results and Discussion

Identification of Screening Hit 2. High-throughput screening resulted in the identification of the amino alcohol **2** as a weak antagonist of the CaR in functional and binding assays (Table 1). Compound **2** was identified from a β-adrenoreceptor antagonist program where it had been shown to be a potent antagonist of the β_2-adrenoreceptor and a potent agonist of the β_1- and β_3-adrenoreceptors. Further selectivity testing of **2** revealed that this basic lipophilic amine, a common pharmacophore for a variety of enzymes, also had affinity for the dopamine (DAT), serotonin (SERT), and norepinephrine (NET) transporters as well as the cytochrome P_{450} 2D6 (CYP2D6) and the cardiac human ether-a-go-go related gene (hERG) ion channel (Table 1).[22,23]

Structure−Activity Studies. The initial focus of the structure activity studies was the optimization of CaR antagonist activity of **2** while also attempting to reduce the affinity of off-target interactions, most notably those on the β-adrenoreceptor family subtypes. Our initial efforts focused on the SAR of the left-hand side benzimidazol-2-one group as detailed in Table 2.

Replacement of the benzimidazol-2-one moiety of **2** with a phenyl group provided analog **7**, which was 5- and 15-fold more potent than **2** in the fluorimetric imaging plate reader (FLIPR) and binding assays, respectively (Table 2). Analog **14**, which incorporates the electron donating 2-methoxyphenyl group, reduced potency in both assays relative to **7**. The left-hand side alkyl analogs **15**−**17** were either less potent or equipotent to the phenyl analog **7** and warranted no further investigation. Extension of the aromatic moiety of **7** by incorporation of a 2-naphthyl group provided analog **8** with improved potency versus the lead analog **7**. Analogs **9** and **10** with an electron withdrawing chlorine group at either the 2 or 3 position of the left-hand side aromatic group resulted in a 4.7- and 2.3-fold increase in antagonist potency in the FLIPR and binding assays, respectively, relative to the unsubstituted aromatic analog **7**. The 2,3-dichloro aromatic analog **11** resulted in a further increase in potency over the monochloro analogs **9** and **10**, suggesting that added electron withdrawing capability and increased lipophilicity results in increased potency. The 2-cyanophenyl analog **12** was essentially equipotent with the 2,3-dichloro analog **11**. Incorporation of both the chlorine and cyano moieties provided **13**, which was the most potent left-hand side aromatic identified in these initial SAR studies. However, assessment of the selectivity of the more potent CaR antagonists **12** and **13** identified during the course of the left-hand side structure−activity studies revealed that, despite substantial increases in antagonist potency versus the CaR, no improvement in off-target interactions were made with either of these analogs relative to the initial screening hit **2** (Table 3).

The structure− activity studies to explore the role of the right-hand side moiety began with holding the left-hand side phenyl group as in analog **7** invariant (Table 4). Initial studies probed the role of the geminal dimethyl group. Removal of the geminal dimethyl group contained within analog **7** provided **20**, which was inactive in both assays. Moving the geminal dimethyl group over one carbon provided analog **21**, which was also inactive. Similarly, analog **22** in which one of the methyl groups was removed was inactive. These results suggest strongly that the geminal dimethyl moiety contained within this amino alcohol template is playing a critical role in antagonist potency through the binding to a hydrophobic pocket within the transmembrane domain of the receptor and/or by imparting a conformational constraint to these receptor antagonists through a classic Thorpe−Ingold effect which serves to increase affinity for the receptor.[24] Indeed, as shown in Figure 2, overlay of the conformations of global energy minima of analogs **7** and **20** shows clearly that analog **20**, lacking the geminal dimethyl

Downloaded by UNIV OF NEWCASTLE on October 11, 2009 | http://pubs.acs.org
Publication Date (Web): June 3, 2009 | doi: 10.1021/jm900364m

Scheme 3. Synthesis of *N*- and *O*-Methylated Analogs **27** and **28**[a]

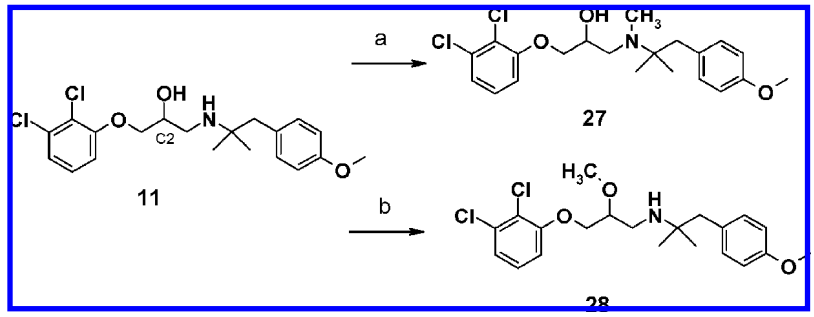

[a] Reagents and conditions: (a) 37% aq CH_2O, $NaCNBH_3$, CH_3OH; (b) DMF, NaH, CH_3I, rt.

Scheme 4. Synthesis of des-Hydroxy Analog **31**[a]

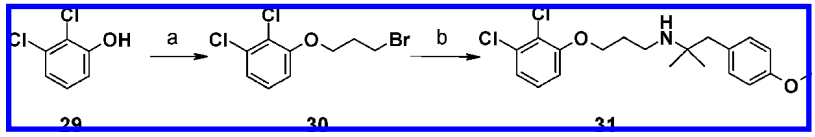

[a] Reagents and conditions: (a) K_2CO_3, 1,3-dibromopropane, 2,3-dichlrorphenol, CH_3CN; (b) **30**, CH_2Cl_2, **4**.

Scheme 5. Synthesis of Chiral Amino Alcohols **32** and **33**[a]

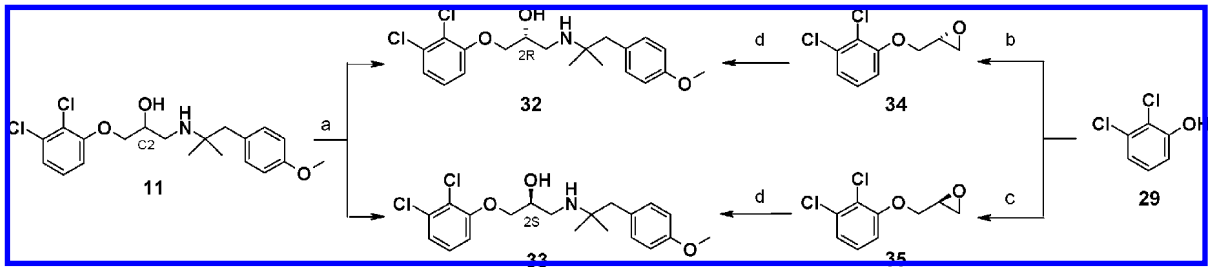

[a] Reagents and conditions: (a) HPLC separation; (b) 2,3-dichlorophenol, acetone, K_2CO_3, (*R*)-nosyl epoxide, reflux; (c) 2,3-dichlorophenol, acetone, K_2CO_3, (*S*)-nosyl epoxide, reflux; (d) **4**, ethanol, reflux.

Scheme 6. Synthesis of Analog **38**[a]

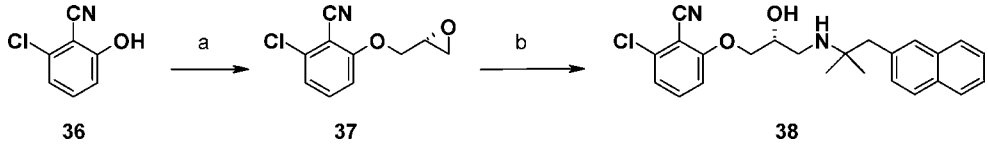

[a] Reagents and conditions: (a) (*R*)-nosyl epoxide, acetone, K_2CO_3, reflux; (b) [1,1-dimethyl-2-(2-naphthalenyl)ethyl]amine, EtOH, reflux.

moiety, is in an extended conformation. In contrast, analog **7**, which contains the geminal dimethyl group, is seen to be in a C-shaped conformation with a $\pi-\pi$ stacking interaction between the pendant aromatic moieties (distance of 3.9 Å between aromatic groups for the energy minimized conformation).[25] Further modeling analysis revealed that the extended conformation of analog **20** is approximately 1.6 kcal higher in energy than the C-shaped conformer, while the extended conformation of analog **22** is approximately 0.3 kcal lower, further suggesting that the geminal dimethyl group is playing a critical role in determining the conformation of analogs such as **7**. Removal of the benzylic methylene group as in analogs **33** resulted in a complete loss in receptor potency versus analog **7**, while addition of another methylene unit as in analog **24** resulted in a loss in potency in the FLIPR assay relative to **7** but were essentially equipotent in the binding assay (Table 4). These data suggest that it is a combination of the spacing between the two pendant aromatic groups and the conformational preference imparted by the geminal dimethyl groups through the Thorpe−Ingold

Table 1. Potencies and Selectivity of the Calcium Receptor Antagonist Lead **2**

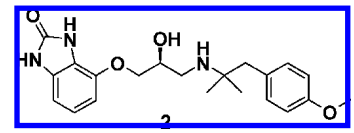

assay	conc (μM)
CaR functional IC_{50}	11.0
CaR binding IC_{50}	31.8
β_2 binding IC_{50}	0.0013
β_1 binding EC_{50}	0.003
β_3 binding EC_{50}	0.007
DAT binding IC_{50}	1.20
SERT binding IC_{50}	0.061
NET binding IC_{50}	0.600
CYP2D6 binding IC_{50}	1.26
hERG binding IC_{50}	11.8

Downloaded by UNIV OF NEWCASTLE on October 11, 2009 | http://pubs.acs.org
Publication Date (Web): June 3, 2009 | doi: 10.1021/jm900364m

Table 2. Potencies of Left-Hand Side Moieties

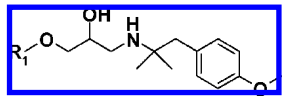

compd	R_1	CaR IC_{50} (μM) FLIPR	binding
2		11[a]	31.8
7	phenyl	2.3	2.3
14	2-methoxyphenyl	15.6	3.5
15	*n*-propyl	16	7.0
16	*i*-propyl	6.4	10
17	*n*-butyl	2.2	3.2
8	2-naphthyl	1.4	1.3
9	2-chlorophenyl	0.49	1.0
10	3-chlorophenyl	0.47	1.0
11	2,3-dichlorophenyl	0.045	0.20
12	2-cyanophenyl	0.058	0.14
13	2-cyano-3-chlorophenyl	0.038	0.070

[a] Functional data.

Table 3. Potencies and Selectivity of the Calcium Receptor Antagonist Hit **2** and Analogs **12** and **13**

assay	IC_{50} or EC_{50}(μM) **2**	**12**	**13**
CaR FLIPR IC_{50}	11.0[a]	0.045	0.038
CaR binding IC_{50}	31.8	0.20	0.070
β_2 binding IC_{50}	0.0013	0.021	0.023
β_1 binding EC_{50}	0.003	NA	NA
β_3 binding EC_{50}	0.007	0.02	NA
DAT binding IC_{50}	1.20	0.30	1.1
SERT binding IC_{50}	0.061	0.021	0.034
NET binding IC_{50}	0.600	0.30	1.0
CYP2D6 binding IC_{50}	1.26	0.036	0.076
hERG binding IC_{50}	11.8	3.5	3.6

[a] Functional data. NA = not active.

Table 4. Potencies of Right-Hand Side Moieties

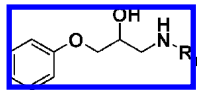

compd	R_1	CaR IC_{50} (μM) FLIPR	binding
7	$C(CH_3)_2CH_2Ph$-*p*-OCH_3	2.3	2.47
20	$(CH_2)_2Ph$-*p*-OCH_3	>100	>10
21	$CH_2C(CH_3)_2Ph$-*p*-OCH_3	>100	>10
22	$CH(CH_3)CH_2Ph$-*p*-OCH_3	>100	>10
23	$C(CH_3)_2Ph$-*p*-OCH_3	>100	>10
24	$C(CH_3)_2(CH_2)_2Ph$-*p*-OCH_3	13	2.78
25	$C(CH_3)_2CH_2Ph$	2.3	NT[a]
26	$C(CH_3)_2CH_2$-2-naphthyl	0.45	0.21

[a] NT = not tested.

effect, which permit these aromatic moieties to form a $\pi-\pi$ stacking interaction that are important contributors to antagonist activity. Removal of the *p*-methoxy moiety to provide **25** resulted in no loss in activity relative to **7**. Analogs **26** with a 2-naphthyl left-hand side amine resulted in an increase in potency in both assays. Here again, as with the SAR studies that examined the left-hand side, the SAR studies that investigated the role of the right-hand side of the amino alcohol-based antagonist template led to improvements in potency over the parent analog **7** with the incorporation of the 2-naphthyl moiety as contained within antagonist **26**. Unfortunately, this modification did not lead to any further increase in the selectivity of

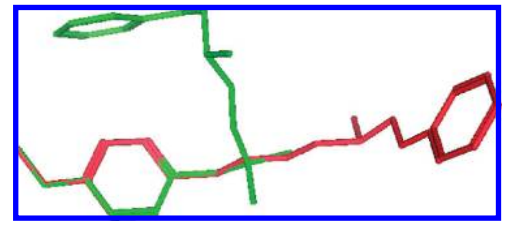

Figure 2. Overlay of the energy minimized structures of **7** (green) and **20** (red).

Table 5. SAR of Propanolamine Linker

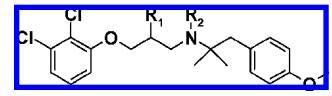

compd	R_1	R_2	CaR IC_{50} (μM) FLIPR	binding
11	OH	H	0.045	0.20
27	OH	CH_3	>3.0	2.3
28	OCH_3	H	>3.0	0.95
31	H	H	2.5	0.93

Table 6. Potencies and Selectivities of the Individual Enantiomers of **11**

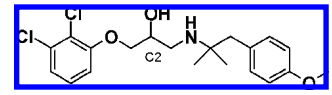

compd	C2 chirality	IC_{50} (μM) CaR FLIPR	CaR binding	β_2 binding	EC_{50} (μM) β_3 binding
11	*R/S*	0.045	0.20	0.021	0.20
32	*R*	0.038	0.068	0.30	NA[a]
33	*S*	0.34	0.30	0.001	0.20

[a] NA = not active.

this analog versus the previously discussed off-target interactions. Antagonist **26** remained a potent inhibitor of the of the monoamine transporters (SERT $IC_{50} = 0.006$ μM, NET $IC_{50} = 0.20$ μM, and DAT $IC_{50} = 0.30$ μM) as well as hERG ($IC_{50} = 1.0$ μM) and CYP2D6 ($IC_{50} = 0.078$ μM). Additionally, no improvement in selectivity versus the β-adrenergic receptors was observed for analog **26** (β_1 and β_3 EC_{50}'s = 0.023 and 0.65 μM, respectively, and β_2 $IC_{50} = 0.40$ μM).

The structure−activity studies focused on the central propanolamine linker were initiated around analog **11**, which was detailed above as a potent antagonist in both the FLIPR and binding assays (Table 5). Methylation of either the hydroxyl group or the secondary amine as in analogs **28** and **27** resulted in a significant loss in potency, suggesting that hydrogens on these atoms are critical for the formation of hydrogen bonds within the receptor active site. Analog **31** in which the hydroxyl group was removed also resulted in a significant loss in antagonist potency relative to analog **11**, further suggesting the critical role of this hydroxyl moiety in facilitating effective interaction with the receptor.

Assessment of the role of the stereochemistry of the C-2 secondary hydroxyl group in determining antagonist potency and selectivity was performed utilizing analog **11**, which as a racemate is a potent CaR antagonist (Table 6). Upon separation of the enantiomers it was shown that the C2 *R* enantiomer **32** was 9- and 4.5-fold more potent than the *S* enantiomer **33** in the FLIPR and binding assays, respectively. These results show that the CaR has a clear stereochemical preference for the *R* enantiomer. This stereochemical preference was recapitulated in vivo in the rat where intravenous injection of the *R*-

Downloaded by UNIV OF NEWCASTLE on October 11, 2009 | http://pubs.acs.org
Publication Date (Web): June 3, 2009 | doi: 10.1021/jm900364m

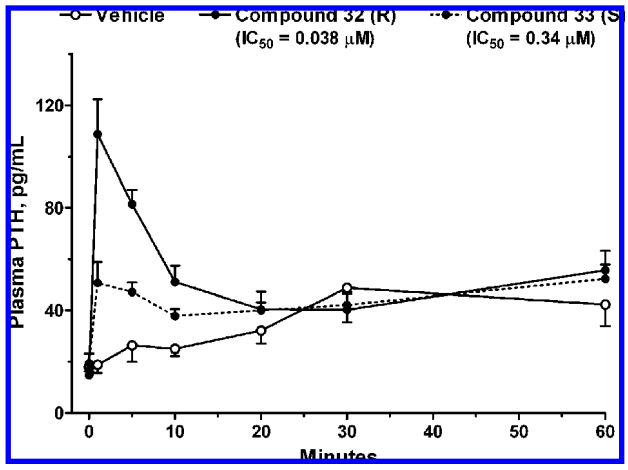

Figure 3. Acute increases in plasma PTH levels following iv injection of CaR antagonists **32** or **33** (10 μmol/kg) in normal conscious rats. Values are mean ± SE, $n = 6$/group. PTH was measured using a rat PTH(1-34) immunoradiometric assay (Immutopics, San Clemente, CA), Note the greater activity of **32** (*R*-enantiomer) compared with **33** (*S*-enantiomer).

Downloaded by UNIV OF NEWCASTLE on October 11, 2009 | http://pubs.acs.org
Publication Date (Web): June 3, 2009 | doi: 10.1021/jm900364m

enantiomer elicited significantly higher levels of PTH over that of the less active *S*-enantiomer (Figure 3). Evaluation of the β-adrenoreceptor selectivity of the individual *R* and *S* enantiomers showed that the *S* enantiomer **33** was 300-fold more potent than the *R* enantiomer **32** as a β_2 adrenoreceptor antagonist. Additionally when evaluated as β_3 adrenoreceptor agonists, the *R* enantiomer **32** was devoid of activity while the *S* enantiomer **33** was active (Table 6). If one assumes that the three-point binding model detailed in the Easson−Stedman hypothesis extends to aryloxyethyl amines such as **32** and **33**, then this stereochemical preference for adrenoreceptor activity is consistent with the plethora of available adrenoreceptor antagonist/agonist literature.[26] It was also encouraging to observe that the stereochemical preference exerted by the CaR upon the amino alcohol antagonist template was opposite to that preferred by the β-adrenergic receptors examined. It is this stereochemical preference that has permitted the disassociation of CaR antagonist activity from β-adrenergic receptor activity present in the initial lead **2**. Unfortunately this stereochemical preference, which led to greater CaR potency and selectivity over the β-adrenergic receptor, did not extend further to selectivity over the monoamine transporters for analog **32** (SERT $IC_{50} = 0.027$ μM, NET $IC_{50} = 0.07$ μM, and DAT $IC_{50} = 1.3$ μM) as well as hERG ($IC_{50} = 2.6$ μM) and CYP2D6 ($IC_{50} = 0.005$ μM).

As detailed above and outlined in Scheme 7, an initial understanding of the structure−activity relationships that exist within the three regions of the amino alcohol antagonist lead **2** led to the identification of the optimal left-hand side aromatic group contained within **13** and the right-hand side aromatic amine within **26** as well as the requisite *R* stereochemistry of the secondary alcohol of the propanolamine linker in **34**. In an effort to further optimize antagonist activity, the critical binding elements contained within **13**, **26**, and **34** were combined to produce analog **38**, which retained potent CaR antagonism. These potencies represent a 255- and 10600-fold increases in antagonist potency for **38** over the lead **2** in the FLIPR and binding assays, respectively (Table 7). Also encouraging was the separation of β-adrenergic receptor activity from CaR antagonist activity with analog **38**, where it was shown to be a 4.3 μM antagonist of the β_2 adrenergic receptor and was devoid of agonist activity at the β_1 or β_3 adrenergic receptors. This represents a 3300-fold improvement in selectivity at the β_2 adrenergic receptor for **38** over the screening lead **2**. Unfortunately, as with several of the analogs detailed above, no improvement in selectivity for the monoamine transporters, the hERG channel, or CYP2D6 were reduced to practice with **38** or any of the other analogs detailed within this manuscript. The small molecule X-ray crystal structure of **38** (Figure 4) shows this molecule to have adopted a C-shaped conformation. This structure further confirms the SAR trends discussed above in that the geminal dimethyl moiety contained within this amino alcohol antagonist template serves to impart a conformational constraint and place the pendant aromatic groups in proximity for a $\pi-\pi$ interaction. This interaction is likely critical for potent antagonism of the CaR.

Pharmacokinetics and Pharmacodynamics of 38. Evaluation of the pharmacokinetics of amino alcohol **38** in the rat showed this compound to have an oral bioavailability of 11% with a high rate of clearance (74 mL/min/kg), a $T_{1/2}$ of 2 h, and volume of distribution of 11.0 L/kg. Undoubtedly, the high volume of distribution of **38** is related to the fact that this molecule is a basic, lipophilic amine that is widely distributed into tissues and likely demonstrates lysosomotropic behavior. As has been previously disclosed and briefly summarized here for context, the efficacy of analog **38** was evaluated in the ovariectomized (OVX) rat model of postmenopausal osteoporosis following five weeks of daily oral administration of a 100 μmol/kg dose.[9] Additionally, in this experiment, the efficacy of **38** was compared directly to the efficacy of a subcutaneously administered dose (5 μg/kg) of rat PTH (1-34). Plasma levels of analog **38** and PTH following oral administration of **38** remained elevated at the 4 h time point. The high volume of distribution of **38** is likely responsible for the prolonged exposure to **38** and the protracted PTH response. In contrast, while the plasma levels of rat PTH (1-34) achieved a similar maximum level to that observed for PTH following administration of **38**, baseline levels had been restored after only 2 h. The differing PTH exposure profiles of orally administered **38** and injected rat PTH (1-34) had markedly different effects on bone. Daily oral administration of **38** for 5 weeks resulted in an increase in both the formation of new bone and the resorption of old bone with no net increase in bone mass. In contrast, treatment with rat PTH (1-34) resulted in increased bone mass. When analog **38** was administered to OVX rats together with continuous subcutaneous infusion of the antiresorptive agent 17β-estradiol, a net increase in bone mass was observed.

Conclusions

In this paper, we have detailed the identification of the high throughput screening lead **2** as a weak antagonist of the CaR with a variety of off-target interactions. Structure−activity studies to optimize the three different portions of this amino alcohol lead in terms of both potency versus the CaR as well as off-target selectivity led to the discovery that the *R*-enantiomer of the C2 alcohol of the propanolamine linker conferred greater CaR antagonist activity with greater selectivity over the β-adrenergic receptor than that of the *S*-enantiomer but did not affect activity in other selectivity counterscreens, most notably the norepinephrine, dopamine, and serotonin monoamine transporters, the hERG ion channel and CYP2D6, all of which share an affinity for lipophilic basic amines. Further optimization efforts led to the identification of analog **38**, a potent CaR antagonist with high clearance, a large volume of distribution, and low oral bioavailability in rats. Analog **38** has been shown to increase bone mass in OVX rats when given in conjunction with the antiresorptive agent 17β-estradiol. To

Table 7. Potencies and Selectivities of **2** and **38**

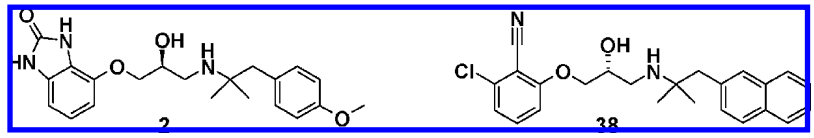

	IC_{50} (μM)								EC_{50} (μM)
compd	CaR FLIPR	CaR binding	SERT binding	NET binding	DAT binding	CYP2D6	hERG binding	β_2 binding	β_1/β_3 binding
2	11.0	31.8	0.061	0.60	1.20	1.26	11.8	0.0013	0.003/0.007
38	0.043	0.003	0.002	0.20	0.20	0.045	3.00	4.3	NA/NA[a]

[a] NA = not active.

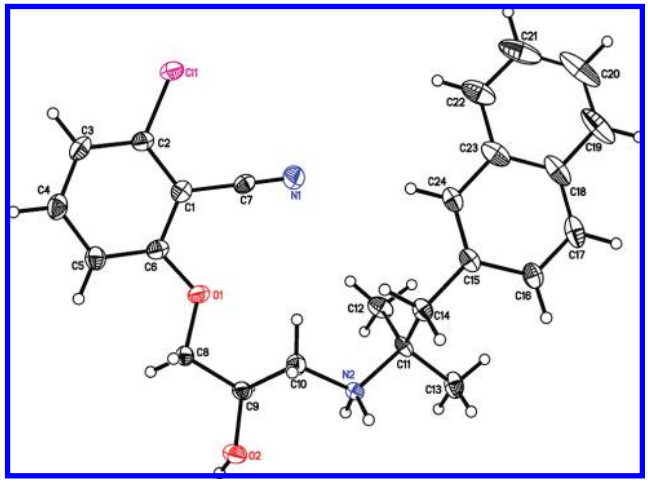

Figure 4. Small molecule X-ray crystal structure of the calcium receptor antagonist **38**.

facilitate new bone growth, the ideal molecule should produce a transient spike of PTH release following oral administration. Efforts to design molecules with this desired pharmacokinetic and pharmacodynamic profile and greater selectivity over the hERG ion channel, monoamine transporters, and CYP2D6 will be the subject of future publications.

Experimental Procedures

Calcium Receptor Inhibitor Assay. HEK 293 4.0-7 cells were constructed as described by Rogers et al.[27] First, 48 h prior to running the CaR assay, frozen HEK293 CaRec4.0-c17 cells were thawed, counted, and diluted to 3×10^5/mL (15K/50 μL). The cell medium used to dilute the cells consisted of DMEM/F12 (HAM'S) 1:1 with L-glutamine, 15 mM HEPES, phenol red, 10% fetal bovine serum, and 1% penicillin−streptomycin solution. Cell solution was seeded at 15K cells/50 μL/well in Greiner poly-D-lysine coated 384-well, black, clear bottom, tissue culture plates and left at room temperature for 1 h to reduce edge effect. After the first hour at room temperature, cell plates were then placed into a 37 °C, 5% CO_2 incubator for 48 h.

On the day of the experiment, plate confluency was first checked by microscope. Wells should be ~100% confluent in an even cell monolayer. Assay reagents were prepared fresh. Dye load buffer consisted of Hank's buffered saline solution with 0.75 mM calcium, without magnesium, without sodium bicarbonate, with 20 mM Hepes, probenecid (2.5 mM final concentration), Fluo4 (2 μM final concentration), and brilliant black (500 μM final concentration). Compound dilution buffer consisted of Hank's buffered saline solution without calcium, without magnesium (without sodium bicarbonate), and CHAPS (0.01% final concentration). A ligand curve plate was also prepared fresh. A 16 point curve was dispensed into a Greiner 384-well polypropylene plate. The top concentration of the ligand CaCl was 2.875 mM (final concentration), and the lowest concentration was 0.375 mM (final concentration). An EC_{80} value was generated from the curve data.

The CaR assay began when the cell media was aspirated from the cell plate using a Tecan plate washer, leaving nothing but the cell monolayer. Dye load buffer is added to the cell plate at 20 μL/well using a multidrop, and the loaded plate was incubated for 45 min at 37 °C, 5% CO_2. Compound plates were received with 1 μL of compound stamped at 5 mM top concentration (25 μM final conc in cell plate). Compound dilution buffer was added to columns 1−24 in the compound plate at 65 μL/well using a Multidrop. Column 6 was prestamped with 1 μL of DMSO to represent the high control, and column 18 received 65 μL of buffer as the low control. The compound addition takes place on a Cybi Well dispenser when 10 μL of diluted compound was added to the dye loaded cell plate. The cell plate with compound was then incubated at room temperature for 5 min.. The antagonist addition took place on the FLIPR when 10 μL of EC_{80} challenge was added to the cell plate and fluorescence imagining proceeded for 65 s. Column 18 of the EC_{80} challenge plate contained only buffer to represent a low control or tool antagonist.

Calcium Receptor Binding Assay. HEK 293 4.0-7 cells stably transfected with the human parathyroid calcium receptor ("HuPCaR") were scaled up in T180 tissue culture flasks. Plasma membrane is obtained by polytron homogenization or glass dounce in buffer (50 mM Tris-HCl pH 7.4, 1 mM EDTA, 3 mM $MgCl_2$) in the presence of a protease inhibitor cocktail containing 1 μM leupeptin, 0.04 μM pepstatin, and 1 mM PMSF. Aliquoted membrane was snap frozen and stored at −80 °C. ^{3}H labeled compound was radiolabeled to a radiospecific activity of 44 Ci/mmol and was aliquoted and stored in liquid nitrogen for radiochemical stability.

A typical reaction mixture contained 2 nM ^{3}H compound ((*R*,*R*)-*N*-4′-methoxy-*t*-3-3′-methyl-1′-ethylphenyl-1-(1-naphthyl)ethylamine), or ^{3}H compound (*R*)-*N*-[2-hydroxy-3-(3-chloro-2-cyanophenoxy)propyl]-1,1-dimethyl-2-(4-methoxyphenyl)ethylamine 4−10 μg membrane in homogenization buffer containing 0.1% gelatin and 10% EtOH in a reaction volume of 0.5 mL. Incubation was performed in 12 × 75 polyethylene tubes in an ice water bath. To each tube, 25 μL of test sample in 100% EtOH was added, followed by 400 μL of cold incubation buffer and 25 μL of 40 nM ^{3}H-compound in 100% EtOH for a final concentration of 2 nM. The binding reaction was initiated by the addition of 50 μL of 80−200 ug/mL HEK 293 4.0-7 membrane diluted in incubation buffer and allowed to incubate at 4 °C for 30 min. Wash buffer was 50 mM Tris-HCl containing 0.1% PEI. Nonspecific binding was determined by the addition of 100-fold excess of unlabeled homologous ligand and was generally 20% of total binding. The binding reaction was terminated by rapid filtration onto 1% PEI pretreated GF/C filters using a Brandel harvester. Filters were placed in scintillation fluid and radioactivity assessed by liquid scintillation counting.

General. Except where indicated, materials and reagents were used as supplied. Nuclear magnetic resonance spectra were recorded at either 250 or 400 MHz using, respectively, a Bruker AM 250 or Bruker AC 400 spectrometer. Mass spectra were taken on a PE Syx API III instruments using electrospray (ES) ionization techniques. Elemental analyses were obtained using a Perkin-Elmer 240C elemental analyzer. Reactions were monitored by TLC analysis using Analtech Silica Gel GF or E. Merck Silica Gel 60

Downloaded by UNIV OF NEWCASTLE on October 11, 2009 | http://pubs.acs.org
Publication Date (Web): June 3, 2009 | doi: 10.1021/jm900364m

Scheme 7. Combination of the SAR Studies Leading to Analog **38**

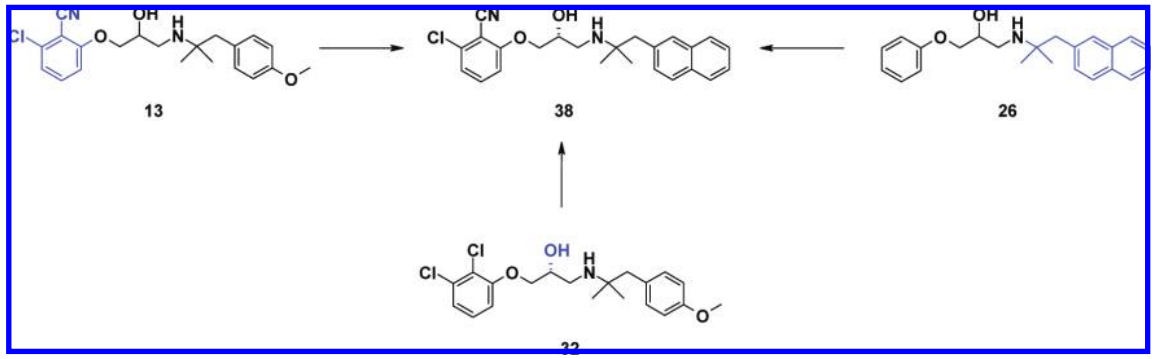

F-254 thin layer plates. Flash chromatography was carried out on E. Merck Kieselgel 60 (230−400 mesh) silica gel. The purity of all tested compounds, which were not analyzed via elemental analysis, were determined by high performance liquid chromatography. Method A: 5−100% acetonitrile:water (with 0.1% TFA) over 18 min with a total run time of 20 min using a 4.6 mm × 50 mm id S-5 mm, YMC Combiscreen ODS column. Method B: 5−100% acetonitrile:water (with 0.1% TFA) over 18 min with a total run time of 20 min using a 4.6 mm × 150 mm id, 5 mm, Zorbax Stablebond C8 column. All compounds analyzed by these methods possessed purities equal to or greater than 95%, with the exception of analog **14**, which is 91.7% pure by method A and 95.8% pure by method B.

(1,1-Dimethyl-2-[4-(methyloxy)phenyl]ethyl)(2-oxiranylmethyl)amine (5). A solution of (1,1-dimethyl-2-[4-(methyloxy)phenyl]ethyl)amine (7.46 g, 41.6 mmol) in isopropyl alcohol (75 mL) was cooled to 0 °C under N_2. Epichlorohydrin (3.2 mL, 40.8 mmol) was added dropwise and reaction stirred at 0 °C for 30 min before warming to room temperature overnight. The reaction was concentrated in vacuo and purified via column chromatography (0−12% CH_3OH/CH_2Cl_2) to provide the title compound (45%). ^{1}H NMR (400 MHz, chloroform-*d*) δ ppm 7.08−7.16 (m, J = 6.25, 6.25, 5.81, 3.92 Hz, 2 H), 6.87 (s, 1 H), 6.82−6.86 (m, 2 H), 3.98 (ddd, J = 11.05, 8.15, 5.31 Hz, 1 H), 3.76−3.83 (m, 3 H), 3.67 (dd, J = 6.32, 4.04 Hz, 1 H), 3.56−3.65 (m, J = 11.24, 9.16, 9.16, 5.31 Hz, 2 H), 2.98 (dd, J = 12.13, 3.79 Hz, 1 H), 2.76−2.82 (m, 1 H), 2.75 (s, 1 H), 1.12−1.20 (m, 6 H).

1-((1,1-Dimethyl-2-[4-(methyloxy)phenyl]ethyl)amino)-3-(phenyloxy)-2-propanol (7). A solution of sodium hydride (95%, 0.116 g, 4.59 mmol) in DMF (6.0 mL) under N_2 was prepared. Phenol (0.433 g, 4.60 mmol) in DMF (6.0 mL) was added and the reaction stirred at room temperature for 15 min (1,1-dimethyl-2-[4-(methyloxy)phenyl]ethyl)(2-oxiranylmethyl)amine (0.354 g, 1.51 mmol) in DMF (4.0 mL) was added and the reaction heated at 100 °C for 20 h. The reaction was cooled and quenched with the addition of H_2O. The aqueous layer was extracted two times with ethyl acetate. The combined organic layers were washed with brine, dried over Na_2SO_4, filtered, and concentrated. Column chromatography (0−10% CH_3OH/CH_2Cl_2) was used to purify. The resulting oil was dissolved in CH_3CN and HCl/Et_2O (1.0 N, 1.5 equiv) was added. The reaction stirred for 10−15 min and concentrated in vacuo to afford the HCl salt of the title compound (38%) as a white solid. ^{1}H NMR (400 MHz, DMSO-d_6) δ ppm 9.01 (s, 1 H), 8.60 (s, 1 H), 7.32 (dd, J = 8.97, 7.20 Hz, 2 H), 7.14 (t, J = 7.96 Hz, 2 H), 6.97 (t, J = 7.96 Hz, 3 H), 6.90 (d, J = 8.59 Hz, 2 H), 5.93 (d, J = 4.04 Hz, 1 H), 4.24 (s, 1 H), 4.03 (d, J = 5.31 Hz, 2 H), 3.74 (s, 3 H), 3.23 (s, 1 H), 3.06 (d, J = 9.60 Hz, 1 H), 2.90−2.99 (m, 2 H), 1.16−1.24 (m, 6 H). MS (ESI) 330.2 $(M + H)^+$.

1-((1,1-Dimethyl-2-[4-(methyloxy)phenyl]ethyl)amino)-3-(2-naphthalenyloxy)-2-propanol (8). The title compound was prepared following the procedure above substituting 2-naphthol for phenol. The title compound (21%) was isolated as a white solid. ^{1}H NMR (400 MHz, DMSO-d_6) δ ppm 9.05 (s, 1 H), 8.64 (s, 1 H), 7.85 (ddd, J = 9.98, 6.69, 5.56 Hz, 3 H), 7.44−7.51 (m, 1 H), 7.37 (td, J = 7.45, 1.01 Hz, 2 H), 7.20−7.25 (m, J = 4.42, 4.42, 4.42, 4.42 Hz, 1 H), 7.14 (t, J = 8.84 Hz, 2 H), 6.90 (d, J = 8.84 Hz, 2 H), 6.00 (d, J = 4.04 Hz, 1 H), 4.30−4.39 (m, 1 H), 4.18 (t, J = 7.71 Hz, 2 H), 3.73 (s, 3 H), 3.31 (s, 1 H), 3.11 (d, J = 9.60 Hz, 1 H), 2.92−3.01 (m, 2 H), 1.17−1.26 (m, 6 H). MS (ESI) 380.2 $(M + H)^+$.

1-[(2-Chlorophenyl)oxy]-3-((1,1-dimethyl-2-[4-(methyloxy)phenyl]ethyl)amino)-2-propanol (9). The title compound was prepared following the procedure above substituting 2-chlorophenol for phenol. The title compound (29%) was isolated as a white solid: ^{1}H NMR (400 MHz, DMSO-d_6) δ ppm 8.93 (s, 1 H), 8.65 (s, 1 H), 7.45 (dd, J = 7.96, 1.64 Hz, 1 H), 7.28−7.38 (m, 1 H), 7.13−7.24 (m, 3 H), 6.99 (td, J = 7.71, 1.26 Hz, 1 H), 6.90 (d, J = 8.84 Hz, 2 H), 5.97 (d, J = 4.29 Hz, 1 H), 4.28 (s, 1 H), 4.08−4.19 (m, 2 H), 3.74 (s, 3 H), 3.32 (d, J = 2.78 Hz, 1 H), 3.12 (d, J = 9.60 Hz, 1 H), 2.89−2.98 (m, 2 H), 1.16−1.25 (m, 6 H). MS (ESI) 364.2 $(M + H)^+$.

1-[(3-Chlorophenyl)oxy]-3-((1,1-dimethyl-2-[4-(methyloxy)phenyl]ethyl)amino)-2-propanol (10). The title compound was prepared following the procedure above substituting 3-chlorophenol for phenol. The title compound (19%) was isolated as a white solid. ^{1}H NMR (400 MHz, DMSO-d_6) δ ppm 8.97 (s, 1 H), 8.59 (s, 1 H), 7.31−7.38 (m, 1 H), 7.15 (d, J = 8.59 Hz, 2 H), 7.06−7.11 (m, 1 H), 7.03 (dd, J = 7.96, 1.14 Hz, 1 H), 6.88−6.99 (m, 3 H), 5.94 (d, J = 4.29 Hz, 1 H), 4.23 (s, 1 H), 4.02−4.10 (m, 2 H), 3.74 (s, 3 H), 3.26 (s, 1 H), 3.05 (d, J = 9.09 Hz, 1 H), 2.89−2.98 (m, 2 H), 1.16−1.24 (m, 6 H). MS (ESI) 364.2 $(M + H)^+$.

1-[(2,3-Dichlorophenyl)oxy]-3-((1,1-dimethyl-2-[4-(methyloxy)-phenyl]ethyl)amino)-2-propanol (11). The title compound was prepared following the procedure above substituting 2,3-dichlorophenol for phenol. The title compound (26%) was isolated as a white solid. ^{1}H NMR (400 MHz, DMSO-d_6) δ ppm 8.93 (s, 1 H), 8.66 (s, 1 H), 7.32−7.40 (m, 1 H), 7.23 (ddd, J = 17.43, 8.34, 1.26 Hz, 2 H), 7.15 (d, J = 8.59 Hz, 2 H), 6.90 (d, J = 8.84 Hz, 2 H), 5.99 (d, J = 4.80 Hz, 1 H), 4.25−4.32 (m, 1 H), 4.13−4.23 (m, J = 11.21, 11.21, 10.17, 5.05 Hz, 2 H), 3.74 (s, 3 H), 3.29 (s, 1 H), 3.11 (d, J = 9.60 Hz, 1 H), 2.90−2.98 (m, 2 H), 1.16−1.24 (m, 6 H). MS (ESI) 398.0/400.0 $[(M/M + 2) + H]^+$.

2-([3-((1,1-Dimethyl-2-[4-(methyloxy)phenyl]ethyl)amino)-2-hydroxypropyl]oxy)benzonitrile (12). The title compound was prepared following the procedure above substituting 2-[4-(methyloxy)phenyl]-2-propanamine for 2-[4-(methyloxy)phenyl]ethanamine and 2-[(2-oxiranylmethyl)oxy]benzonitrile for 2-[(phenyloxy)methyl]oxirane. The title compound (82%) was isolated as an off white solid. ^{1}H NMR (400 MHz, DMSO-d_6) δ ppm 8.92−9.16 (m, 1 H), 8.71 (br s, 1 H), 7.64−7.81 (m, 2 H), 7.32 (d, J = 8.59 Hz, 1 H), 7.02−7.25 (m, 3 H), 6.90 (d, J = 8.84 Hz, 2 H), 6.02 (br s, 1 H), 4.11−4.39 (m, 2 H), 3.59−3.83 (m, 2 H), 3.25−3.50 (m, 4 H), 3.13 (q, J = 9.18 Hz, 1 H), 2.81−3.03 (m, 1 H), 1.22 (s, 6 H). MS (ESI) 355.2 $(M + H)^+$.

2-Chloro-6-([3-((1,1-dimethyl-2-[4-(methyloxy)phenyl]ethyl)-amino)-2-hydroxypropyl]oxy)benzonitrile (13). The title compound was prepared following the procedure above substituting 2-cyano-3-chlorophenol for phenol. The title compound (19%) was isolated as a white solid. ^{1}H NMR (400 MHz, DMSO-d_6) δ ppm 9.04 (s, 1 H), 8.72 (s, 1 H), 7.71 (t, J = 8.34 Hz, 1 H), 7.38 (s, 1

Downloaded by UNIV OF NEWCASTLE on October 11, 2009 | http://pubs.acs.org
Publication Date (Web): June 3, 2009 | doi: 10.1021/jm900364m

Downloaded by UNIV OF NEWCASTLE on October 11, 2009 | http://pubs.acs.org
Publication Date (Web): June 3, 2009 | doi: 10.1021/jm900364m

H), 7.32 (dd, $J = 8.34, 3.28$ Hz, 1 H), 7.13 (d, $J = 4.04$ Hz, 2 H), 6.90 (d, $J = 8.84$ Hz, 2 H), 6.05 (s, 1 H), 4.29 (td, $J = 10.23, 3.79$ Hz, 3 H), 3.74 (s, 3 H), 3.29 (s, 1 H), 3.13 (s, 1 H), 2.90−2.99 (m, 2 H), 1.16−1.25 (m, 6 H). MS (ESI) 389.0 $(M + H)^+$.

1-((1,1-Dimethyl-2-[4-(methyloxy)phenyl]ethyl)amino)-3-([2-(methyloxy)phenyl]oxy)-2-propanol (14). The title compound was prepared following the procedure above substituting guaiacol for phenol. The title compound (20%) was isolated as a white solid. ^{1}H NMR (400 MHz, DMSO-d_6) δ ppm 8.92 (s, 1 H), 8.59 (s, 1 H), 7.13 (d, $J = 6.82$ Hz, 2 H), 6.98−7.05 (m, $J = 10.24, 3.69, 3.56, 3.56, 3.45, 1.52$ Hz, 2 H), 6.87−6.96 (m, $J = 14.27, 7.71, 7.33, 4.04$ Hz, 4 H), 5.91 (s, 1 H), 4.19−4.27 (m, 1 H), 3.96−4.07 (m, 2 H), 3.71−3.79 (m, 6 H), 3.27 (d, $J = 10.11$ Hz, 1 H), 3.07 (d, $J = 9.60$ Hz, 1 H), 2.89−2.98 (m, 2 H), 1.15−1.25 (m, 6 H). MS (ESI) 360.2 $(M + H)^+$.

1-((1,1-Dimethyl-2-[4-(methyloxy)phenyl]ethyl)amino)-3-(propyloxy)-2-propanol (15). The title compound was prepared following the procedure above substituting *n*-propanol for phenol. The title compound (19%) was isolated as a white solid. ^{1}H NMR (400 MHz, DMSO-d_6) δ ppm 8.85 (s, 1 H), 8.45 (s, 1 H), 7.09−7.17 (m, 2 H), 6.90 (d, $J = 8.84$ Hz, 2 H), 5.64 (s, 1 H), 3.99 (ddd, $J = 10.61, 6.82, 5.81$ Hz, 1 H), 3.74 (s, 3 H), 3.45 (d, $J = 5.31$ Hz, 1 H), 3.43 (d, $J = 5.05$ Hz, 1 H), 3.33 (m, 1 H), 3.11 (d, $J = 2.78$ Hz, 1 H), 3.08 (s, 1 H), 2.85−2.95 (m, 3 H), 1.47−1.56 (m, $J = 7.20, 7.04, 7.04, 7.04, 7.04$ Hz, 2 H), 1.15−1.21 (m, 6 H), 0.87 (t, $J = 7.33$ Hz, 3 H). MS (ESI) 296.2 $(M + H)^+$.

1-((1,1-Dimethyl-2-[4-(methyloxy)phenyl]ethyl)amino)-3-[(1-methylethyl)oxy]-2-propanol (16). The title compound was prepared following the procedure above substituting isopropyl alcohol for phenol. The title compound (29%) was isolated as a white solid. ^{1}H NMR (400 MHz, DMSO-d_6) δ ppm 8.96 (s, 1 H), 8.49 (s, 1 H), 7.11−7.19 (m, 2 H), 6.90 (d, $J = 8.59$ Hz, 2 H), 5.61 (s, 1 H), 3.92−4.02 (m, 1 H), 3.71−3.77 (m, 3 H), 3.58 (dt, $J = 12.13, 6.06$ Hz, 1 H), 3.42−3.46 (m, 1 H), 3.33−3.40 (m, 1 H), 3.10 (t, $J = 10.99$ Hz, 1 H), 2.96 (s, 1 H), 2.84−2.94 (m, $J = 9.22, 9.22, 7.71, 7.20$ Hz, 2 H), 1.15−1.21 (m, 6 H), 1.09 (t, $J = 6.57$ Hz, 6 H). MS (ESI) 296.2 $(M + H)^+$.

1-(Butyloxy)-3-((1,1-dimethyl-2-[4-(methyloxy)phenyl]ethyl)-amino)-2-propanol (17). The title compound was prepared following the procedure above substituting *n*-butanol for phenol. The title compound (29%) was isolated as a white solid. ^{1}H NMR (400 MHz, DMSO-d_6) δ ppm 9.04 (s, 1 H), 8.53 (s, 1 H), 7.11−7.19 (m, 2 H), 6.90 (d, $J = 8.84$ Hz, 2 H), 3.97−4.06 (m, $J = 6.47, 6.47, 6.19, 5.62, 4.80$ Hz, 1 H), 3.67−3.76 (m, 3 H), 3.47−3.58 (m, 2 H), 3.39 (ddd, $J = 7.07, 3.92, 3.66$ Hz, 1 H), 3.35 (d, $J = 6.06$ Hz, 1 H), 3.09 (t, $J = 10.99$ Hz, 1 H), 2.85−2.97 (m, $J = 13.55, 8.46, 7.01, 6.85$ Hz, 3 H), 1.49 (td, $J = 10.67, 6.69$ Hz, 2 H), 1.33 (ddd, $J = 19.58, 12.76, 4.55$ Hz, 3 H), 1.15−1.24 (m, 6 H), 0.89 (t, $J = 7.33$ Hz, 3 H). MS (ESI) 310.2 $(M + H)^+$.

2-[(Phenyloxy)methyl]oxirane (18). Potassium carbonate (15.1 g, 109 mmol) and epichlorohydrin (21 mL, 268 mmol) were added to a solution of phenol (5.05 g, 53.7 mmol) and CH_3CN. The flask was sealed and heated at reflux for 3 days. The reaction was cooled to room temperature, filtered, washed with ethyl acetate, and concentrated. Column chromatography (0−30% ethyl acetate: hexane) provided 6.08 g (76%) of **18** as an oil. ^{1}H NMR (400 MHz, chloroform-*d*) δ ppm 7.32 (dd, $J = 8.84, 7.33$ Hz, 1 H), 7.28 (s, 1 H), 6.92−7.03 (m, 3 H), 4.24 (dd, $J = 10.86, 3.28$ Hz, 1 H), 3.99 (dd, $J = 10.99, 5.68$ Hz, 1 H), 3.33−3.45 (m, $J = 6.09, 3.66, 2.95, 2.95$ Hz, 1 H), 2.93 (d, $J = 4.29$ Hz, 1 H), 2.79 (dd, $J = 4.93, 2.65$ Hz, 1 H).

1-((2-[4-(Methyloxy)phenyl]ethyl)amino)-3-(phenyloxy)-2-propanol (20). 2-[(Phenyloxy)methyl]oxirane (**18**) (0.639 g, 4.26 mmol) in ethanol (8.5 mL) was added to 2-[4-(methyloxy)phenyl]ethanamine (0.640 g, 4.23 mmol) and the reaction heated at 80 °C in a sealed flask for 20 h. The reaction was cooled to room temperature and concentrated in vacuo. Column chromatography (0−10% CH_3OH:CH_2Cl_2) produced 0.563 g (39%) of **20** as an off-white solid. ^{1}H NMR (400 MHz, DMSO-d_6) δ ppm 9.11 (br s, 1 H), 8.90 (br s, 1 H), 7.30 (d, $J = 8.08$ Hz, 1 H), 7.24−7.37 (m, 1 H), 7.18 (d, $J = 8.59$ Hz, 2 H), 6.87−6.99 (m, 5 H), 5.92 (d, $J = 5.05$ Hz, 1 H), 4.24 (ddd, $J = 8.91, 4.36, 4.17$ Hz, 1 H), 3.98 (quin, $J = 4.74$ Hz, 2 H), 3.73 (s, 3 H), 3.15 (t, $J = 11.62$ Hz, 2 H), 3.19 (d, $J = 19.96$ Hz, 1 H), 3.05 (d, $J = 9.85$ Hz, 1 H), 2.90−2.98 (m, $J = 11.64, 6.32, 5.23, 4.61, 4.04$ Hz, 2 H). MS (ESI) 302.2 $(M + H)^+$.

1-((2-Methyl-2-[4-(methyloxy)phenyl]propyl)amino)-3-(phenyloxy)-2-propanol (21). The title compound was prepared following the procedure above substituting 2-methyl-2-[4-(methyloxy)-phenyl]-1-propanamine for 2-[4-(methyloxy)phenyl]ethanamine. The title compound (50%) was isolated as a white solid. ^{1}H NMR (400 MHz, DMSO-d_6) δ ppm 8.43 (br s, 2 H), 7.37 (d, $J = 8.84$ Hz, 2 H), 7.30 (dd, $J = 8.59, 7.33$ Hz, 2 H), 6.92 (d, $J = 8.59$ Hz, 4 H), 6.87−6.98 (m, 1 H), 5.91 (d, $J = 4.80$ Hz, 1 H), 4.27 (d, $J = 3.28$ Hz, 1 H), 3.86−3.99 (m, $J = 10.11, 8.91, 8.91, 5.18$ Hz, 2 H), 3.74 (s, 3 H), 3.25 (br s, 2 H), 3.10 (br s, 1 H), 2.95 (t, $J = 10.99$ Hz, 1 H), 1.41 (s, 6 H). MS (ESI) 330.2 $(M + H)^+$.

1-((1-Methyl-2-[4-(methyloxy)phenyl]ethyl)amino)-3-(phenyloxy)-2-propanol (22). The title compound was prepared following the procedure above substituting 1-[4-(methyloxy)phenyl]-2-propanamine for 2-[4-(methyloxy)phenyl]ethanamine. The title compound (20%) was isolated as a white solid. ^{1}H NMR (400 MHz, DMSO-d_6) δ ppm 9.13 (br s, 1 H), 8.76 (br s, 1 H), 7.31 (dd, $J = 8.59, 7.33$ Hz, 2 H), 7.17 (d, $J = 7.58$ Hz, 2 H), 6.87−7.00 (m, 6 H), 5.94 (br s, 1 H), 4.27 (d, $J = 4.29$ Hz, 1 H), 4.00 (d, $J = 4.80$ Hz, 2 H), 3.94−4.06 (m, 1 H), 3.73 (s, 3 H), 3.41 (d, $J = 10.11$ Hz, 2 H), 3.37 (br s, 2 H), 3.28 (br s, 1 H), 3.22 (ddd, $J = 8.91, 4.11, 3.41$ Hz, 2 H), 3.11 (br s, 1 H), 3.08 (d, $J = 9.35$ Hz, 1 H), 2.61 (dddd, $J = 10.52, 5.31, 4.04, 3.63$ Hz, 1 H), 1.12 (t, $J = 6.69$ Hz, 3 H). MS (ESI) 316.2 $(M + H)^+$.

1-((1-Methyl-1-[4-(methyloxy)phenyl]ethyl)amino)-3-(phenyloxy)-2-propanol (23). The title compound was prepared following the procedure above substituting 2-[4-(methyloxy)phenyl]-2-propanamine for 2-[4-(methyloxy)phenyl]ethanamine. The title compound (66%) was isolated as a white solid. ^{1}H NMR (400 MHz, DMSO-d_6) δ ppm 9.51 (br s, 1 H), 9.10 (br s, 1 H), 7.59 (m, $J = 8.84$ Hz, 2 H), 7.27 (dd, $J = 8.59, 7.33$ Hz, 2 H), 6.99 (m, $J = 8.84$ Hz, 2 H), 6.93 (t, $J = 7.33$ Hz, 1 H), 6.86 (d, $J = 7.83$ Hz, 2 H), 5.82 (d, $J = 4.80$ Hz, 1 H), 4.14 (td, $J = 6.63, 3.16$ Hz, 1 H), 3.84−3.95 (m, $J = 5.34, 5.34, 5.12, 4.67$ Hz, 2 H), 3.77 (s, 3 H), 2.77 (t, $J = 10.74$ Hz, 1 H), 2.51−2.63 (m, 1 H), 1.73 (d, $J = 2.02$ Hz, 6 H). MS (ESI) 316.2 $(M + H)^+$.

1-((1,1-Dimethyl-3-[4-(methyloxy)phenyl]propyl)amino)-3-(phenyloxy)-2-propanol (24). The title compound was prepared following the procedure above substituting 2-methyl-4-[4-(methyloxy)phenyl]-2-butanamine for 2-[4-(methyloxy)phenyl]ethanamine. The title compound (58%) was isolated as a white solid. ^{1}H NMR (400 MHz, DMSO-d_6) δ ppm 9.00 (br s, 1 H), 8.57 (br s, 1 H), 7.31 (dd, $J = 8.72, 7.20$ Hz, 2 H), 7.15 (m, $J = 8.59$ Hz, 2 H), 6.97 (d, $J = 7.07$ Hz, 3 H), 6.86 (m, 2 H), 5.90 (d, $J = 4.80$ Hz, 1 H), 4.16−4.28 (m, 1 H), 4.02 (d, $J = 5.56$ Hz, 2 H), 3.72 (s, 3 H), 3.11−3.24 (m, 1 H), 2.97 (d, $J = 9.60$ Hz, 1 H), 2.56 (ddd, $J = 7.71, 5.18, 4.29$ Hz, 2 H), 1.88 (ddd, $J = 7.52, 5.56, 4.36$ Hz, 2 H), 1.37 (s, 6 H). MS (ESI) 344.2 $(M + H)^+$.

1-([1,1-Dimethyl-2-(2-naphthalenyl)ethyl]amino)-3-(phenyloxy)-2-propanol (26). The title compound was prepared following the procedure above substituting 2-methyl-1-(2-naphthalenyl)-2-propanamine for 2-[4-(methyloxy)phenyl]ethanamine. The title compound (57%) was isolated as a white solid. ^{1}H NMR (400 MHz, DMSO-d_6) δ ppm 9.16 (br s, 1 H), 8.73 (br s, 1 H), 7.90 (t, $J = 3.92$ Hz, 2 H), 7.88 (s, 1 H), 7.78 (s, 1 H), 7.46−7.56 (m, $J = 6.38, 4.83, 4.06, 4.06, 3.41, 2.02$ Hz, 2 H), 7.40 (dd, $J = 8.34, 1.52$ Hz, 1 H), 7.24−7.37 (m, 2 H), 6.98 (t, $J = 4.17$ Hz, 2 H), 6.92−7.03 (m, 1 H), 5.96 (d, $J = 4.80$ Hz, 1 H), 4.29 (d, $J = 3.79$ Hz, 1 H), 4.05 (d, $J = 5.31$ Hz, 2 H), 3.30 (br s, 1 H), 3.21 (d, $J = 2.02$ Hz, 2 H), 3.12 (d, $J = 9.60$ Hz, 1 H), 1.30 (s, 6 H). MS (ESI) 350.2 $(M + H)^+$.

1-[(2,3-Dichlorophenyl)oxy]-3-[(1,1-dimethyl-2-[4-(methyloxy)-phenyl]ethyl)(methyl)amino]-2-propanol (27). Formaldehyde (37% aq, 1.8 mL, 22.2 mmol) and $NaCNBH_3$ (0.360 g, 5.73 mmol) were added to a solution of 1-[(2,3-dichlorophenyl)oxy]-3-((1,1-dimethyl-2-[4-(methyloxy)phenyl]ethyl)amino)-2-propanol (**11**, 0.580 g, 1.46

Downloaded by UNIV OF NEWCASTLE on October 11, 2009 | http://pubs.acs.org
Publication Date (Web): June 3, 2009 | doi: 10.1021/jm900364m

mmol) in CH_3OH (15 mL) under N_2. The reaction was stirred at room temperature for 5 days. Dilution with H_2O was followed by extraction with CH_2Cl_2 two times. The combined organic layers were washed with brine, dried over Na_2SO_4, filtered, and concentrated. Column chromatography (0−10% CH_3OH:CH_2Cl_2) followed by evaporation of solvent in the presence of HCl (1.0 M in Et_2O) produced 0.592 g (91%) of **27** as a white solid. ^{1}H NMR (400 MHz, DMSO-d_6) δ ppm 9.44 (br s, 1 H), 7.36 (t, J = 8.21 Hz, 1 H), 7.23 (dd, J = 14.27, 8.46 Hz, 2 H), 7.19 (d, J = 8.34 Hz, 2 H), 6.91 (d, J = 8.59 Hz, 2 H), 6.08 (d, J = 3.79 Hz, 1 H), 5.97 (br s, 1 H), 4.38 (q, J = 7.07 Hz, 1 H), 4.23 (s, 1 H), 4.20 (q, J = 5.39 Hz, 2 H), 3.74 (s, 3 H), 3.67 (br s, 1 H), 3.61 (br s, 1 H), 3.02−3.10 (m, 1 H), 2.98 (br s, 1 H), 2.86−2.94 (m, 3 H), 2.34 (s, 1 H), 1.25 (d, J = 12.88 Hz, 6 H). MS (ESI) 412.0/414.0 [(M/M + 2) + H]$^+$.

[3-[(2,3-Dichlorophenyl)oxy]-2-(methyloxy)propyl](1,1-dimethyl-2-[4-(methyloxy)phenyl]ethyl)amine (28). To a solution of 1-[(2,3-dichlorophenyl)oxy]-3-((1,1-dimethyl-2-[4-(methyloxy)phenyl]ethyl)amino)-2-propanol (**11**, 0.612 g, 1.54 mmol) in DMF (15 mL) under N_2 were added sodium hydride (95%, 0.048 g, 1.90 mmol) and iodomethane (0.12 mL, 1.92 mmol). The reaction was stirred at room temperature for 5 days. Dilution with ethyl acetate was followed by washes with H_2O, 0.5 M HCl, and brine. The organic layer was dried over Na_2SO_4, filtered, and concentrated. Column chromatography (0−10% CH_3OH:CH_2Cl_2) followed by evaporation of solvent in the presence of HCl (1.0 M in Et_2O) gave 0.336 g (49%) of **28** as a white solid. ^{1}H NMR (400 MHz, DMSO-d_6) δ ppm 9.26 (br s, 1 H), 8.57 (br s, 1 H), 7.37 (d, J = 8.34 Hz, 1 H), 7.18−7.29 (m, 1 H), 7.24 (td, J = 10.99, 7.58 Hz, 2 H), 7.14 (m, J = 8.59 Hz, 2 H), 6.90 (m, J = 8.59 Hz, 2 H), 4.42 (dd, J = 10.74, 3.66 Hz, 1 H), 4.22 (dd, J = 10.61, 4.55 Hz, 1 H), 4.10 (dd, J = 8.72, 3.66 Hz, 1 H), 3.74 (s, 3 H), 3.51 (s, 3 H), 3.36 (br s, 1 H), 3.18 (d, J = 9.60 Hz, 1 H), 2.95 (s, 2 H), 1.22 (s, 6 H). MS (ESI) 412.0/414.0 [(M/M + 2) + H]$^+$.

3-Bromopropyl 2,3-Dichlorophenyl Ether (30). Potassium carbonate (1.76 g, 12.7 mmol) and 1,3-dibromopropane (0.96 mL, 9.40 mmol) were added to a solution of 2,3-dichlorophenol (**29**, 0.512 g, 3.14 mmol) in CH_3CN (25 mL). The reaction was stirred at 70 °C for 24 h. Upon cooling, the reaction was filtered, washed with CH_3CN, and concentrated. Column chromatography (0−15% ethyl acetate:hexane) provided 0.115 g (13%) of **30** as an oil. ^{1}H NMR (400 MHz, chloroform-d) δ ppm 7.15 (q, J = 7.16 Hz, 1 H), 7.09 (ddd, J = 7.89, 3.85, 3.66 Hz, 1 H), 6.90 (dd, J = 8.21, 1.39 Hz, 1 H), 4.30 (t, J = 5.94 Hz, 2 H), 4.20 (t, J = 5.68 Hz, 1 H), 3.69 (t, J = 6.32 Hz, 1 H), 2.31−2.42 (m, J = 5.81, 5.81, 5.68, 5.43 Hz, 2 H).

(3-[(2,3-Dichlorophenyl)oxy]propyl)(1,1-dimethyl-2-[4-(methyloxy)phenyl]ethyl)amine (31). To a solution of **30** (0.115 g, 0.405 mmol) in CH_2Cl_2 (1.1 mL) was added (1,1-dimethyl-2-[4-(methyloxy)phenyl]ethyl)amine (0.080 g, 0.447 mmol). The reaction mixture was stirred at room temperature for 18 h then at reflux for 4 days. The reaction was cooled and concentrated in vacuo. Column chromatography (0−10% CH_3OH:CH_2Cl_2) followed by evaporation of solvent in the presence of HCl (1.0 M in Et_2O) afforded 0.047 g (28%) of **31** as a white solid. ^{1}H NMR (400 MHz, DMSO-d_6) δ ppm 8.95 (br s, 2 H), 7.36 (t, J = 8.21 Hz, 1 H), 7.21 (dd, J = 18.44, 4.29 Hz, 1 H), 7.17−7.30 (m, 1 H), 7.16 (d, J = 8.59 Hz, 2 H), 6.89 (d, J = 8.59 Hz, 2 H), 4.39 (q, J = 7.07 Hz, 1 H), 4.25 (t, J = 5.94 Hz, 2 H), 3.74 (s, 3 H), 3.17 (br s, 1 H), 2.92 (s, 1 H), 2.35 (s, 1 H), 2.21 (d, J = 6.82 Hz, 1 H), 1.35 (t, J = 7.07 Hz, 1 H), 1.22 (s, 6 H). MS (ESI) 382.0/384.0 [(M/M + 2) + H]$^+$.

(2*R*)-2-([(2,3-Dichlorophenyl)oxy]methyl)oxirane (34). To a solution of 2,3-dichlorophenol (**29**, 1.03 g, 6.29 mmol) in acetone (20 mL) was added K_2CO_3 (2.61 g, 18.9 mmol) and the reaction mixture was heated at reflux for 30 min. The reaction was cooled, (*R*)-nosyl epoxide (1.63 g, 6.31 mmol) was added, and reaction heated at reflux for 3 days. The reaction was cooled, filtered, rinsed with acetone, and concentrated in vacuo. Column chromatography (0−30% ethyl acetate:hexane) afforded 1.27 g (92%) of **34** as a clear oil. ^{1}H NMR (400 MHz, chloroform-d) δ ppm 7.15 (dq, J = 7.33, 7.16 Hz, 1 H), 7.11 (s, 1 H), 6.89 (dd, J = 7.83, 1.77 Hz, 1 H), 4.34 (dd, J = 11.24, 2.91 Hz, 1 H), 4.07 (dd, J = 11.12, 5.31 Hz, 1 H), 3.42 (dddd, J = 5.56, 3.79, 3.41, 2.40 Hz, 1 H), 2.95 (d, J = 4.04 Hz, 1 H), 2.86 (dd, J = 4.93, 2.65 Hz, 1 H).

(2*S*)-2-([(2,3-Dichlorophenyl)oxy]methyl)oxirane (35). The title compound was prepared following the procedure above substituting (*S*)-nosyl epoxide for (*R*)-nosyl epoxide. The title compound (96%) was isolated as a clear oil. ^{1}H NMR (400 MHz, chloroform-d) δ ppm 7.15 (dt, J = 14.21, 7.17 Hz, 1 H), 7.11 (s, 1 H), 6.89 (dd, J = 7.83, 1.77 Hz, 1 H), 4.34 (dd, J = 11.24, 2.91 Hz, 1 H), 4.07 (dd, J = 11.12, 5.31 Hz, 1 H), 3.42 (dddd, J = 6.44, 3.03, 2.78, 2.65 Hz, 1 H), 2.95 (d, J = 4.29 Hz, 1 H), 2.86 (dd, J = 5.05, 2.53 Hz, 1 H).

(2*R*)-1-[(2,3-Dichlorophenyl)oxy]-3-((1,1-dimethyl-2-[4-(methyloxy)phenyl]ethyl)amino)-2-propanol (32). (2*R*)-2-([(2,3-Dichlorophenyl)oxy]methyl)oxirane (**34**, 0.44 g, 2.03 mmol) was added to a solution of (1,1-dimethyl-2-[4-(methyloxy)phenyl]ethyl)-amine (**4**, 0.359 g, 2.00 mmol) in ethanol (4.2 mL) and heated at reflux for 2 days. The reaction was cooled and concentrated in vacuo. Column chromatography (0−10% CH_3OH:CH_2Cl_2) followed by evaporation of solvent in the presence of HCl (1.0 M in Et_2O) provided 0.593 g (67%) of **32** as a white solid. ^{1}H NMR (400 MHz, DMSO-d_6) δ ppm 8.93 (br s, 1 H), 8.65 (br s, 1 H), 7.36 (t, J = 8.21 Hz, 1 H), 7.24 (ddd, J = 12.95, 8.40, 4.17 Hz, 2 H), 7.15 (m, J = 8.59 Hz, 2 H), 6.90 (m, J = 8.59 Hz, 2 H), 5.98 (d, J = 4.80 Hz, 1 H), 4.29 (t, J = 6.19 Hz, 1 H), 4.12−4.25 (m, J = 11.24, 11.24, 10.11, 5.05 Hz, 2 H), 3.74 (s, 3 H), 3.32 (d, J = 1.77 Hz, 1 H), 3.11 (d, J = 9.85 Hz, 1 H), 2.94 (s, 2 H), 1.22 (s, 6 H). MS (ESI) 398.0/400.0 [(M/M + 2) + H]$^+$.

(2*S*)-1-[(2,3-Dichlorophenyl)oxy]-3-((1,1-dimethyl-2-[4-(methyloxy)phenyl]ethyl)amino)-2-propanol (33). The title compound was prepared following the procedure above substituting (2*S*)-2-([(2,3-dichlorophenyl)oxy]methyl)oxirane (**35**). The title compound (60%) was isolated as a white solid. ^{1}H NMR (400 MHz, DMSO-d_6) δ ppm 8.98 (br s, 1 H), 8.68 (br s, 1 H), 7.35 (d, J = 8.08 Hz, 1 H), 7.24 (ddd, J = 12.19, 8.15, 4.17 Hz, 2 H), 7.15 (m, J = 8.59 Hz, 2 H), 6.90 (m, J = 8.59 Hz, 2 H), 5.99 (d, J = 4.80 Hz, 1 H), 4.30 (t, J = 6.19 Hz, 1 H), 4.12−4.24 (m, J = 10.96, 10.96, 10.17, 5.05 Hz, 2 H), 3.74 (s, 3 H), 3.30 (d, J = 12.63 Hz, 2 H), 3.15 (br s, 1 H), 3.11 (d, J = 9.60 Hz, 1 H), 2.94 (s, 2 H), 1.22 (s, 6 H). MS (ESI) 398.0/400.0 [(M/M + 2) + H]$^+$.

2-Chloro-6-([(2*R*)-2-oxiranylmethyl]oxy)benzonitrile (37). A mixture of 2-chloro-6-fluorobenzonitrile (40.17 g, 258 mmol), 18-crown-6 (22.7 g, 86 mmol), and potassium *tert*-butoxide (38 g, 387 mmol) in acetonitrile (350 mL) was heated at reflux under argon overnight, whereupon 100 mL of 5 N NaOH was added and the mixture was allowed to stir for 1 h. The acetonitrile was removed under vacuum, and the resulting alkaline solution was extracted twice with Et_2O. The aqueous phase was then adjusted to pH = 4 and extracted twice with Et_2O. The organic extract from the acidified aqueous phase was dried over $MgSO_4$, filtered, and concentrated to yield 23.8 g (60%) of 2-chloro-6-hydroxybenzonitrile as a solid. ^{1}H NMR (400 MHz, $CDCl_3$-d) δ ppm 7.38 (t, J = 8.21 Hz, 1 H), 7.04 (d, J = 7.58 Hz, 1 H), 6.96 (d, J = 8.59 Hz, 1 H), 3.65 (br s, 1 H).

To a solution of 2-chloro-6-hydroxybenzonitrile (0.45 g, 2.93 mmol) in acetone (30 mL, 0.1 M) was added potassium carbonate (1.21 g, 8.79 mmol). The resulting mixture stirred at reflux for 30 min. After cooling to room temperature, (2*R*)-2-oxiranylmethyl 3-nitrobenzenesulfonate (0.76 g, 2.93 mmol) was added. The reaction mixture was then heated to reflux and stirred overnight at that temperature. After cooling to room temperature, the reaction mixture was filtered, and the filtrate was concentrated for FCC purification (10−50% EtOAc/Hex). 2-Chloro-6-([(2*R*)-2-oxiranylmethyl]oxy)benzonitrile was obtained as a white solid (0.48 g, 79% yield). ^{1}H NMR (400 MHz, $CDCl_3$-d) δ ppm 7.45 (t, J = 8.34 Hz, 1 H), 7.11 (d, J = 8.08 Hz, 1 H), 6.95 (d, J = 8.34 Hz, 1 H), 4.41 (dd, J = 11.49, 2.91 Hz, 1 H), 4.13 (dd, J = 11.37, 5.31 Hz, 1 H), 3.41 (dt, J = 4.11, 2.62 Hz, 1 H), 2.95 (t, J = 4.42 Hz, 1 H), 2.86 (dd, J = 4.80, 2.53 Hz, 1 H). LCMS m/z = 232 (M + Na$^+$).

2-Chloro-6-[((2*R*)-3-([1,1-dimethyl-2-(2-naphthalenyl)ethyl]-amino)-2-hydroxypropyl)oxy]benzonitrile hydrochloride (38). A solution of 2-chloro-6-([(2*R*)-2-oxiranylmethyl]oxy)benzonitrile (**37**,

0.30 g, 1.43 mmol) and [1,1-dimethyl-2-(2-naphthalenyl)ethyl]-amine (0.28 g, 1.43 mmol) in anhydrous ethanol (7.2 mL, 0.2 M) was heated to reflux overnight. After cooling to room temperature, the reaction mixture was concentrated and purified by column chromatography (1% CH_3OH/CH_2Cl_2) to give pure product. The resulting amine was treated with HCl in Et_2O and subsequently dried under vacuum to generate the title compound as a white solid in the form of an HCl salt (0.54 g, 85%). ^{1}H NMR (400 MHz, $CDCl_3$-*d*) δ ppm 7.75−7.88 (m, 3H), 7.65 (s, 1H), 7.45 (t, J = 4.17 Hz, 2H), 7.40−7.52 (m, 1H), 7.35 (dd, J = 8.46, 1.64 Hz, 1H), 7.09 (d, J = 8.08 Hz, 1H), 6.91 (d, J = 8.59 Hz, 1H), 4.15 (dd, J = 4.80, 2.78 Hz, 2H), 4.05 (dd, J = 6.44, 4.67 Hz, 1H), 3.09 (dd, J = 12.00, 4.42 Hz, 1H), 2.96 (d, J = 6.82 Hz, 1H), 2.93 (d, J = 2.27 Hz, 2H), 2.44 (br s, 2H), 1.19 (s, 3H), 1.18 (s, 3H). LCMS m/z = 409 ($M + H^+$). Elemental anal. calcd: 64.72% C, 5.88% H, 6.29% N; found: 64.52% C, 5.70% H, 6.28% N.

Acknowledgment. We thank Drs. John Gleason and Brian Metcalf for their support of this work.

Supporting Information Available: X-ray crystallographic data for antagonist **38** as well as HPLC purities with two separate conditions for antagonists **7**−**11**, **13**−**17**, **21**−**24**, **26**−**28**, and **31**−**33**. This material is available free of charge via the Internet at http://pubs.acs.org.

References

(1) Iqbal, J.; Inzerillo, A. M.; Moonga, B. S.; Baljit, S.; Zaidi, M. The molecular pharmacology of osteoporosis. *Osteoporosis* **2003**, 569–594.

(2) Deal, C. Osteoporosis therapies: bisphosphonates, SERMS, PTH and new therapies. *Clin. Rev. Bone Miner. Metab*. **2005**, *3*, 125–141. Rodan, G. A.; Martin, T. J. Therapeutic approaches to bone diseases. *Science* **2000**, *289*, 1508–1514.

(3) Bodenner, D.; Redman, C.; Riggs, A. Teriparatide in the management of osteoporosis. *Clin. Interventions Aging* **2007**, *2*, 499–507. Bilezikian, J. P. Anabolic therepy for osteoporosis. *Women's Health* **2007**, *3*, 243–253. Girotra, M.; Rubin, M. R.; Bilezikian, J. P. The use of parathyroid hormone in the treatment of osteoporosis. *Rev. Endocrinol. Metab. Disorders* **2006**, *7*, 113–121. Eriksen, E. F.; Robins, D. A. Teriparatide: a bone formation treatment for osteoporosis. *Drugs Today* **2004**, *40*, 935–948. Quattrocchi, E.; Kourlas, H. Teriparaitide: a review. *Clin. Ther*. **2004**, *26*, 841–854. Dobnig, H. A review of teriparatide and its clinical efficacy in the treatment of osteoporosis. *Expt Opin. Pharmacother*. **2003**, *57*, 710–718. Ebling, P. R.; Russell, R. G. G. Teriparaitide (rhPTH1-34) for the treatment of osteoporosis. *Int. J. Clin. Pract.* **2003**, *57*, 710–718. Berg, C.; Neumeyer, K.; Kirkpatrick, P. Fresh from the pipline: Teriparatide. *Nat. Rev. Drug Discovery*. **2003**, *2*, 257–258.

(4) Kronenberg, H. M. PTHrP and skeletal development. *Ann. New York Acad. Sci*. **2006**, *1068*, 1–13. Murray, T. M.; Rao, L. G.; Divieti, P.; Bringhurst, F. R. Parathyroid hormone secretion and action: evidence for discrete receptors for the carboxyl-terminal region and related biological actions of carboxyl-terminal ligands. *Endocr. Rev.* **2005**, *26*, 78–113. Gardella, T. J.; Juppner, H. Molecular properties of the PTH/PTHrP receptor. *Trends Endocr. Metab.* **2001**, *12*, 210–217. Juppner, H. Receptors for parathyroid hormone and parathyroid hormone-related peptide: exploration of their biological importance. *Bone* **1999**, *25*, 87–90.

(5) Brown, E. M.; MacLeod, R. J. Extracellular Calcium Sensing and Extracellular Calcium Signaling. *Physiol. Rev*. **2001**, *81*, 239–297. Nemeth, E. F. Calcium receptor-dependent regulation of cellular functions. *News Physiol. Sci.* **1995**, *10*, 1–5. Brown, E. M.; MacLeod, R. J. Extracellular calcium sensing and extracellular calcium signaling. *Physiol. Rev.* **2001**, *81*, 239–297. Chen, R. A.; Goodman, W. G. Role of the calcium-sensing receptor in parathyroid gland physiology. *Am. J. Physiol. Renal Physiol.* **2004**, *286*, F1005–F1011. Tfelt-Hansen, J.; Brown, E. M. The calcium-sensing receptor in normal physiology and pathophysiology: a review. *Crit. Rev. Clin. Lab. Sci.* **2005**, *42*, 35–70.

(6) Nemeth, E. F. Misconceptions about calcimimetics. *Anns. N. Y. Acad. Sci*. **2006**, *1068*, 471–476. Nemeth, E. F.; Fox, J. Compounds acting on the parathyroid calcium receptor as novel therapies for hyperparathyroidism and osteoporosis. *Endocr. Updates* **2003**, *19*, 173–202. Nemeth, E. F. Pharmacological regulation of parathyroid hormone secretion. *Curr. Pharm. Des.* **2002**, *8*, 2077–2087. Nemeth, E. F.; Fox, J. Calcimimetic compounds: a direct approach to controlling plasma levels of parathyroid hormone in hyperparathyroidism. *Trends Endocrinol. Metab.* **1999**, *10*, 66–71. Nemeth, E. F.; Bennett, S. A. Tricking the parathyroid gland with novel calcimimetic agents. *Nephrol., Dial., Transplant.* **1998**, *13*, 1923.

(7) Locatelli, F.; Pontoriero, G.; Limbardo, M.; Tentori, F. Cinacalcet hydrochloride: calcimimnetic for the treatment of hyperparathyroidism. *Exp. Opin. Endocr. Metab*. **2006**, *1*, 167–179. Dong, B. J. Cinacalcet: an oral calcimimetic agent for the management of hyperparathyroidism. *Clin. Ther.* **2005**, *27*, 1725–1751. de Francisco, A. L. M. Cinacalcet HCL: a novel therapeutic for the treatment of hyperparathyroidism. *Exp. Opin. Pharmacother.* **2005**, *6*, 441–452.

(8) Nemeth, E. F.; Delmar, E. C.; Heaton, W. L.; Miller, M. A.; Lambert, L. D.; Conklin, R. L.; Gowen, M.; Gleason, J. G.; Bhatnagar, P. K.; Fox, J. Calcilytic compounds: Potent and selective Ca^{+2} receptor. antagonists that stimulate secretion of parathyroid hormone. *J. Pharm. Exp. Ther*. **2001**, *299*, 323–331.

(9) Gowen, M.; Stroup, G. B.; Dodds, R. A.; James, I. E.; Votta, B. J.; Smith, B. R.; Bhatnagar, P. K.; Lago, A. M.; Callahan, J. F.; Del Mar, E. G.; Miller, M. A.; Nemuth, E. F.; Fox, J. Antagonizing the parathyroid calcium receptor stimulates parathyroid secretion and bone formation in osteopenic rats. *J. Clin. Invest*. **2000**, *105*, 1595–1604.

(10) Arey, B. J.; Seethala, R.; Ma, Z.; Fura, A.; Morin, J.; Swartz, J.; Vyas, V.; Yang, W., Jr.; Feyen, J. H. M. A Novel Calcium-Sensing Receptor Antagonist Transiently Stimulates Parathyroid Hormone Secretion in Vivo. *Endocrinology* **2005**, *5*, 1131–1136.

(11) Dauban, P.; Ferry, S.; Faure, H.; Ruat, M.; Dodd, R. H. N^1-Arylsulfonyl-N^2-(1-aryl)ethyl-3-phenylpropane-1,2-diamines as Novel Calcimimetics Acting on the Calcium Sensing Receptor. *Bioorg. Med. Chem. Lett*. **2000**, *10*, 2001–2004.

(12) Kessler, A.; Faure, H.; Ruat, M.; Dauban, P.; Dodd, R. H. N^2-Benzyl-N^1-(1-(1-naphthyl)ethyl)-3-phenylpropane-1,2-diamines and conformationally constrained indole analogs: development of calindol as a new calcimimetic acting at the calcium sensing receptor. *Bioorg. Med. Chem. Lett.* **2004**, *14*, 3345–3349.

(13) Kessler, A.; Faure, H.; Roussanne, M. C.; Ferry, S.; Ruat, M.; Dauben, P.; Dodd, R. H. N^1-Arylsulfonyl-N^2-(1-(1-naphthyl)ethyl)-1,2-diaminocyclohexanes: A New Class of Calcilytic Agents Acting at the Calcium-Sensing Receptor. *ChemBioChem* **2004**, *5*, 1131–1136.

(14) Arey, B. J.; Seethala, R.; Ma, Z.; Fura, A.; Morin, J.; Swartz, J.; Vyas, V.; Yang, W., Jr.; Feyen, J. H. M. A Novel Calcium-Sensing Receptor Antagonist Transiently Stimulates Parathyroid Hormone Secretion in Vivo. *Endocrinology* **2005**, *5*, 1131–1136.

(15) Yang, W.; Wang, Y.; Roberge, J. Y.; Ma, Z.; Liu, Y.; Lawerence, R. M.; Rotella, D. P.; Seethala, R.; Feyen, J. H. M.; Dickson, J. K., Jr. Discovery and structure−activity relationships of benzylpyrrolidine substituted aryloxypropanols as calcium-sensing receptor antagonists. *Bioorg. Med. Chem. Lett*. **2005**, *15*, 1225–1228.

(16) Gavai, A. V.; Vaz, R. J.; Mikkilineni, A. B.; Roberge, J. Y.; Liu, Y.; Lawrence, R. M.; Corte, J. R.; Yang, W.; Bednarz, M.; Dickson Jr, J. K.; Ma, Z.; Seethala, R.; Feyen, J. H. M. Discovery nof novel 1-arylmethyl pyrrolidin-2-yl ethanol amines as calcium-sensing receptor antagonists. *Bioorg. Med. Chem. Lett.* **2005**, *15*, 5478–5482.

(17) Shcherbakova, I.; Balandrin, M. F.; Fox, J.; Ghatak, A.; Heaton, W.; Conklin, R. L. 3*H*-Quinazolin-4-ones as a new calcilytic template for the potential treatment of osteoporosis. *Bioorg. Med. Chem. Lett.* **2005**, *15*, 1557–1560.

(18) Shcherbakova, I.; Huang, G.; Geoffroy, O. J.; Nair, S. K.; Swierczek, K.; Balandrin, M. F.; Fox, J.; Heaton, W. L.; Conklin, R. L. *Bioorg. Med. Chem. Lett*. **2005**, *15*, 2537–2540.

(19) Dobnig, H.; Turner, R. T. Evidence that intermittent treatment with parathyroid hormone increases bone formation in adult rats by activation of bone lining cells. *Endocrinology* **1995**, *136*, 3632–3638. Ishizuya, T.; Yokose, S.; Hori, M.; Noda, T.; Suda, T.; Yoshiki, S.; Yamaguchi, A. Parathyroid hormone exerts disparate effects on osteoclast differentiation depending on exposure time in rat osteoblastic cells. *J. Clin. Invest.* **1997**, *99*, 2961–2970. Frolik, C. A.; Black, E. C.; Cain, R. L.; Satterwhite, J. H.; Brown-Augsburger, P. L.; Sato, M.; Hock, J. M. Anabolic and catabolic bone effects of human parathyroid hormone (1-34) are predicted by duration of hormone exposure. *Bone* **2003**, *33*, 372–379. Onyia, J. E.; Helvering, L. M.; Gelbert, L.; Wei, T.; Huang, S.; Chen, P.; Dow, E. R.; Maran, A.; Zhang, M.; Lotinun, S.; Halladay, D. L.; Miles, R. R.; Kulkarni, N. H.; Ambrose, E. M.; Ma, Y. L.; Frolik, C. A.; Sato, M.; Bryant, H. U.; Turner, R. T. Molecular profile of catabolic versus anabolic treatment regimens of parathyroid hormone (PTH) in rat bone: an analysis of DNA microarray. *J. Cell. Biochem.* **2005**, *95*, 403–418.

(20) Fraher, L. J.; Klein, K.; Marier, R.; Freeman, D.; Hendy, G. N.; Glotzman, D.; Hodsman, A. B. Comparison of the pharmacokinetics of parenteral parathyroid hormone-(1−34) [PTH-(1-34)] and PTH-related peptide-(1-34) in healthy young humans. *J. Clin. Endocr. Metab*. **1995**, *80*, 60–64. Revel, L.; Sorbera, L. A.; Martin, L. Teriparatide: treatment of osteoporosis parathyroid hormone analog. *Drugs Future* **2000**, *25*, 803–808.

Downloaded by UNIV OF NEWCASTLE on October 11, 2009 | http://pubs.acs.org
Publication Date (Web): June 3, 2009 | doi: 10.1021/jm900364m

(21) Nemeth, E. F.; Steffey, M. E.; Hammerland, L. G.; Hung, B. C. P.; van Wagenen, B. C.; DelMar, E. G.; Balandrin, M. F. Calcimimetics with potent and selective activity on the parathyroid calcium receptor. *Proc. Natl. Acad. Sci. U.S.A.* **1998**, *95*, 4040–4045.

(22) Crivori, P.; Poggesi, I. Predictive model for identifying potential CYP2D6 Inhibitors. *Basic Clin. Pharm. Toxicol.* **2005**, *96*, 251–253. Ekins, S.; Gianpaolo, B.; Binkley, S.; Gillespie, J. S.; Ring, B. J.; Winkel, J. H.; Wrighton, S. A. Three- and four dimensional-quantitative structure−activity relationship (3D/4D-QSAR) analyses of CYP2D6 inhibitors. *Pharmacogenetics* **1999**, *9*, 477–489. De Groot, M. J.; Ackland, M. J.; Horne, V. A.; Alex, A. A.; Jones, B. C. Novel approach to predicting P450-mediated drug metabolism: development of a combined protein and pharmacophore model for CYP2D6. *J. Med. Chem.* **1999**, *42*, 1515–1524. Rowland, P.; Blaney, F. E.; Smyth, M. G.; Jones, J. J.; Leydon, V. R.; Oxbrow, A. K.; Lewis, C. J.; Tennant, M. G.; Modi, S.; Eggleston, D. S.; Chenery, R. J.; Bridges, A. M. Crystal structure of the human cytochrome P450 2D6. *J. Biol. Chem.* **2006**, *281*, 7614–7622.

(23) Mitcheson, J. S. hERG potassium channels and the structural basis of drug-induced arrhythmias. *Chem. Res. Toxicol.* **2008**, *21*, 1005–1010. Kramer, C.; Beck, B.; Kriegel, J. M.; Clark, T. A composite model for hERG blockade. *ChemMedChem* **2008**, *3*, 254–265. Stansfeld, P. J.; Gedeck, P.; Gosling, M.; Cox, B.; Mitcheson, J. S.; Sutcliffe, M. J. Drug block of the hERG potassium channel: insights from modeling. *Proteins: Struct., Funct., Bioinf.* **2007**, *68*, 568–580. Sanguinetti, M. C.; Tristani-Firouzi, M. hERG potassium channels and cardiac arrhythmia. *Nature* **2006**, *440*, 463–469. Sanguinetti, M. C.; Mitcheson, J. S. Predicting drug−hERG channel interactions that cause acquired long QT syndrome. *Trends Pharmacol. Sci.* **2005**, *26*, 119–124. Fernandez, D.; Ghanta, A.; Kauffman, G. W.; Sanguinetti, M. C. Physiochemical features of the hERG channel binding site. *J. Biol. Chem.* **2004**, *279*, 10120–10127.

(24) Tonioli, C.; Crisma, M.; Formaggio, F.; Peggion, C. Control of peptide conformation by the Thorpe-Ingold effect (C-α tetrasubstitution). *Biopolymers* **2001**, *60*, 396–419.

(25) The conformational search of global energy minima for analogs **7** and **22** were carried out using the BatchMin module in Maestro. The conformational space was explored by 2000 iterations of Monte Carlo multiple minimum (MCMM) torsional angle sampling procedure in BatchMin, and the energy of each conformation was determined by the OPLS-2005 force field in GB/SA water solvation model.

(26) Easson, L. H.; Stedman, E. Studies on the relationship between chemical constitution and physiological action. V. Molecular dissymmetry and physiological activity. *Biochem. J.* **1933**, *31*, 1257–1266. Testa, B. Mechanisms of chiral recognition in pharmacology. *Acta Pharm. Nord.* **1990**, *2*, 137–143. Ruffolo, Jr., R. R. Chirality in α-and β-adrenoreceptor agonists and antagonists. *Tetrahedron* **1991**, *47*, 9953–9980.

(27) Rogers, K.; Dunn, C.; Hebert, S.; Brown, E.; Nemeth, E. Pharmacological comparison of bovine parathyroid, human parathyroid, and rat kidney calcium receptors expressed in HEK 293 cells. *J. Bone Miner. Res.* **1995**, *10* (Suppl. 1), S483.

JM900364M

Downloaded by UNIV OF NEWCASTLE on October 11, 2009 | http://pubs.acs.org
Publication Date (Web): June 3, 2009 | doi: 10.1021/jm900364m